Postcranial anatomy of *Yinlong downsi* (Dinosauria: Ceratopsia) from the Upper Jurassic Shishugou Formation of China and the phylogeny of basal ornithischians

Fenglu Han, Catherine A. Forster, Xing Xu & James M. Clark

Check for updates

Postcranial anatomy of *Yinlong downsi* (Dinosauria: Ceratopsia) from the Upper Jurassic Shishugou Formation of China and the phylogeny of basal ornithischians

Fenglu Han[a,b]*, Catherine A. Forster[c], Xing Xu[b] and James M. Clark[c]

[a]*School of Earth Sciences, China University of Geosciences, Wuhan, PR China;* [b]*Key Laboratory of Evolutionary Systematics of Vertebrates, Institute of Vertebrate Paleontology and Paleoanthropology, Chinese Academy of Sciences, PR China;* [c]*Department of Biological Sciences, The George Washington University, Washington DC, USA*

Ceratopsia includes some of the best-known ornithischian dinosaurs. Many species are erected based on cranial elements alone, and the postcranial skeletons are either missing or undescribed in many taxa. Here we provide the first detailed postcranial description of *Yinlong downsi* based on the holotype and eight other well-preserved skeletons. *Yinlong downsi* from the early Late Jurassic Shishugou Formation of the Wucaiwan area, Xinjiang, China, represents one of the most basal ceratopsians. The detailed study of the postcranial skeleton reveals one feature unique to it among ceratopsians: a blade-like prepubic process of the pubis with an elongate notch near its ventral margin. The postcranial material of *Yinlong* shares some unique features with that of the ornithischian *Stenopelix valdensis* from the Early Cretaceous of Germany, and provides further evidence that the latter is a basal ceratopsian. A comprehensive phylogenetic analysis of basal ornithischians was built based on 72 taxa and 380 characters. Most of the characters are illustrated for the first time in order to clarify character states. The new ornithischian phylogeny confirms that *Yinlong* belongs to Chaoyangsauridae. Chaoyangsaurids and *Psittacosaurus* form a monophyletic group that is sister to all other ceratopsians. The new phylogeny also supports *Stenopelix valdensis* as a basal ceratopsian, and *Mosaiceratops* to be close to Coronosauria. Additionally, the new phylogeny agrees with other recent analyses that place heterodontosaurids as the most basal ornithischians rather than with marginocephalians. Furthermore, *Isaberrysaura*, which has been hypothesized to be a basal ornithopod, is recovered as one of the most basal stegosaurs for the first time. The former 'hypsilophodontid' taxa are recovered within Ornithopoda rather than outside Cerapoda, and Jeholosauridae is shown to be valid in this analysis.

Keywords: Ceratopsia; Ornithischia; phylogeny; Jurassic; China

Introduction

Numerous basal ceratopsians discovered in China in recent years have helped to clarify the origin and early evolution of the group (Zhao *et al.* 1999, 2006; Xu *et al.* 2002, 2006; Han *et al.* 2015; Zheng *et al.* 2015). However, phylogenetic relationships among basal ceratopsians are still controversial. *Yinlong downsi* was originally recovered as the most basal ceratopsian (Xu *et al.* 2006; Butler *et al.* 2011), and more recently assigned to the Chaoyangsauridae with *Chaoyangsaurus*, *Xuanhuaceratops* and *Hualianceratops* (Han *et al.* 2015; He *et al.* 2015). Other phylogenetic analyses suggest that *Psittacosaurus* represents the most basal taxon (Morschhauser 2012). *Psittacosaurus* was usually considered to differ from neoceratopsians on the basis of many unique features, and is more closely related to neoceratopsians than are *Yinlong* and chaoyangsaurids (He *et al.* 2015; Zheng *et al.* 2015). However, a new phylogeny of ceratopsians

supports the monophyly of chaoyangsaurids and *Psittacosaurus* (Han *et al.* 2015). As a result, new discoveries make the systematic positions of *Psittacosaurus* and other basal ceratopsians more complicated and uncertain than previously thought.

Yinlong downsi was thought to provide additional evidence for the monophyly of Marginocephalia and Heterodontosauridae (Xu *et al.* 2006), but all recent phylogenies of Ornithischia do not support this hypothesis (Butler *et al.* 2008; Makovicky *et al.* 2011; Han *et al.* 2012; Boyd 2015). However, recent ornithischian phylogenies have mainly focused on basal ornithopods with only a few ceratopsians included (Boyd 2015). Here, we provide a new comprehensive analysis of basal ornithischians that includes more basal ceratopsians in order to clarify the position of *Yinlong* and *Psittacosaurus*, and also the relationship between heterodontosaurids and marginocephalians.

For many ceratopsians the postcranial skeleton is missing, described superficially, or undescribed, such as the

---

basal ceratopsians *Chaoyangsaurus*, *Hualianceratops* and *Xuanhuaceratops* (Zhao *et al.* 1999, 2006). In other basal ceratopsians, complete and detailed postcranial information is available, including *Psittacosaurus* (Sereno 1990, 2010), *Auroraceratops* (Morschhauser 2012), *Leptoceratops* (Sternberg 1951) and *Protoceratops* (Brown & Schlaikjer 1940). The postcranial elements of *Psittacosaurus* and Neoceratopsia are significantly different from one another, but the lack of character information from the postcrania of many basal ceratopsians restricts their utility in helping resolve relationships among basal taxa. *Yinlong downsi* is one of the most complete basal ceratopsians and includes well-preserved postcranial elements which have only been briefly described (Xu *et al.* 2006). Here, we provide a detailed postcranial description of *Yinlong downsi*. This information will be significant for characterizing the basal condition of postcrania within Ceratopsia and also the relationships of basal ornithischians.

Institutional abbreviations

IVPP: Institute of Vertebrate Paleontology and Paleoanthropology, Beijing, China; **NHMUK**: Natural History Museum, London, UK; **SAM-PK**: Iziko South African Museum, Cape Town, South Africa.

Systematic palaeontology

Order **Ornithischia** Seeley, 1887
Suborder **Ceratopsia** Marsh, 1890
Family **Chaoyangsauridae** Zhao *et al.*, 2006
Genus *Yinlong* Xu *et al.*, 2006

Type species. *Yinlong downsi* (monotypic).

Diagnosis. As for the type species (see below).

Locality and horizon. Wucaiwan area, Junggar basin, Xinjiang Uyghur Autonomous Region, North-West China. The holotype and referred specimens are from the upper part of the Shishugou Formation. The entire formation is placed in the Oxfordian stage of the early Late Jurassic (Han *et al.* 2016).

Yinlong downsi Xu *et al.*, 2006
(Figs 1–14)

Emended diagnosis. A basal ceratopsian diagnosed by the following autapomorphies: a distinct fossa along the midline of the frontals; a slit-like carotid canal bordered by laminae; premaxillary teeth with a vertical wear facet and a basal shelf; a deep sulcus on the ventral surface of the quadratojugal; large oval nodules concentrated on the lateral surface of the jugal; a squamosal with an expanded dorsal surface and a long, constricted quadrate process; a

strongly craniodorsally extending scapula shaft; and a blade-like prepubic process of the pubis with elongate notch at the base. Cranial characters are described in detail in Han *et al.* (2016).

Holotype. IVPP V14530, a nearly complete skull with mandible and nearly complete postcranial skeleton. The latter is exposed only in dorsal view, and is missing the distal end of the tail and parts of the right forelimb (see Han *et al.* 2016; Supplemental Appendix 1).

Referred material. IVPP V18636, IVPP V18686, IVPP V18637 and IVPP V18684 are associated with cranial elements and were mentioned in a previous study (Han *et al.* 2016); all specimens except IVPP 18637, which is incompletely prepared, are illustrated in Supplemental Appendix 1. More material is included in this study (Supplemental Appendix 1). The measurements of the appendicular skeleton and limbs are given in Supplemental Appendix 2.

IVPP V18679. This partial specimen is disarticulated and consists of postcranial elements including the right humerus; both ulnae and radii; left ilium and complete right ischium.

IVPP V18685. This specimen is larger than the holotype, and only the postcranial elements are preserved, including articulated dorsal vertebrae, sacral vertebrae and 40 articulated caudal vertebrae; the nearly complete left forelimb consists of left scapula, ulna, radius, manus; the paired ilia; the left femur, tibia, fibula and pes.

IVPP V18682. A nearly complete postcranial skeleton, which includes dorsal vertebrae, sacral vertebrae and caudal vertebrae associated with chevrons; paired ilia; left tibia, fibula and partial pes; ossified tendons are present on the neural spine of the dorsal vertebrae.

IVPP V18677. This is the smallest specimen and only preserves the caudal part of the postcranial skeleton in dorsal view, including sacrals, caudals; both ilia; the complete left hind limb; right femur, tibia, fibula and metatarsals (only the proximal ends exposed).

Locality and horizon. As for the genus.

Description and comparisons

Axial skeleton

Cervical series. The cervical vertebrae are well preserved in IVPP V18636 and IVPP V18686, and disarticulated in IVPP V18637, IVPP V14530 and IVPP V18684 (Fig. 1). *Yinlong* has nine cervical vertebrae based on IVPP V18636 (Fig. 1E). This is similar to *Psittacosaurus* (Sereno 1990) and most other basal ornithischians (Han *et al.* 2012), whereas neoceratopsians usually possess more than nine cervicals, such as *Auroraceratops* with 13 cervicals (Morschhauser 2012). The number is usually
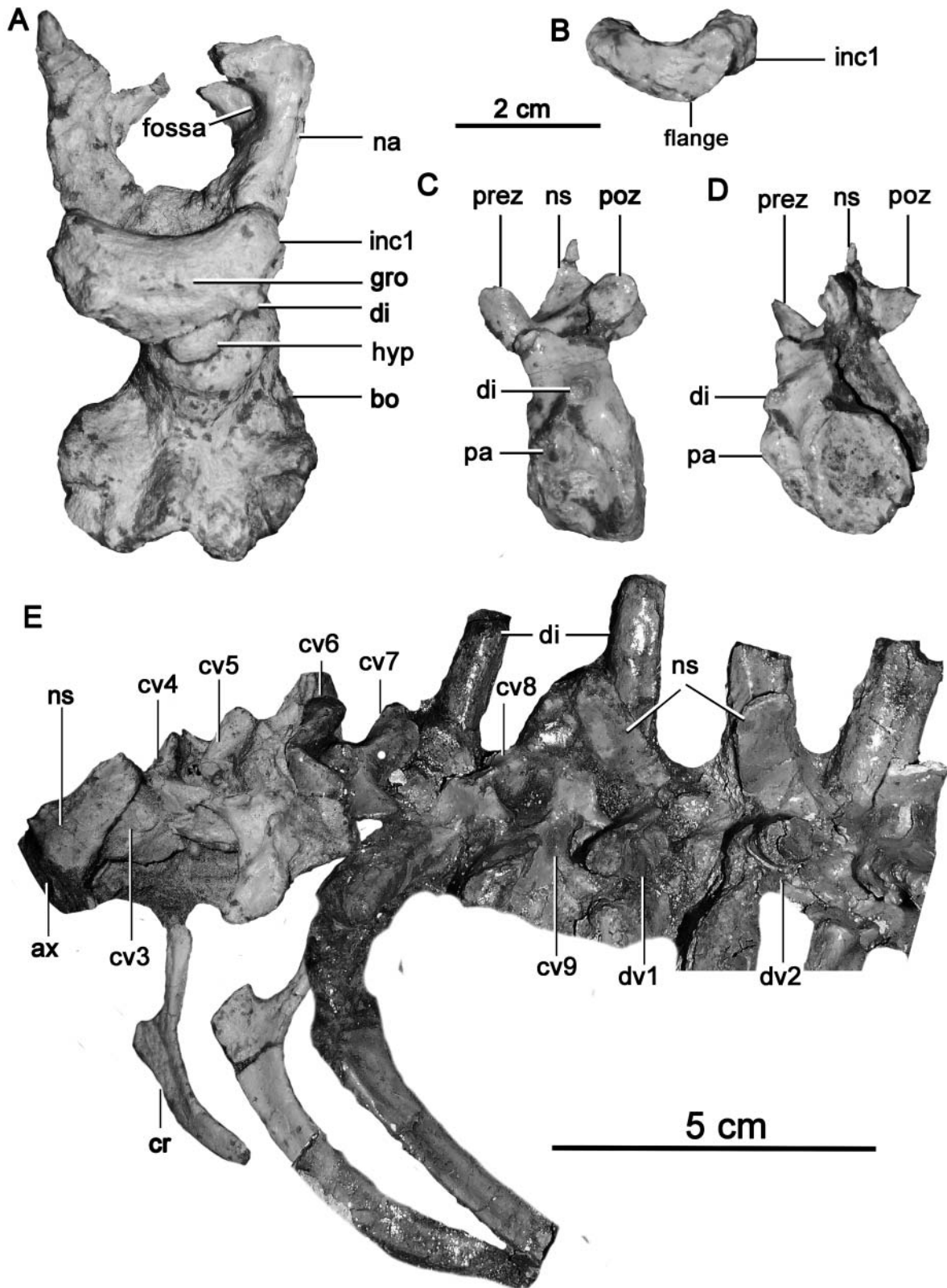
Figure 1. Photographs of the cervical and rostral dorsal vertebrae of *Yinlong downsi*. **A,** IVPP V18637, atlas in caudal view. **B–D,** IVPP V18684; **B,** atlas intercentrum in cranial view; **C,** postaxial cervical in lateral view; **D,** same cervical as C in caudal view. **E,** IVPP V18636 in dorsolateral view. Abbreviations: ax, axis; bo, basioccipital; cr, cervical rib; cv, cervical vertebra; di, diapophysis; dr, dorsal rib; dv, dorsal vertebrate; gro, groove; hyp, hypocentrum; inc1, intercentrum one; na, neural arch; ns, neural spine; pa, parapophysis; prez, prezygapophysis; poz, postzygapophysis.

fewer than nine in basal thyreophorans, such as *Scelidosaurus* (six, Norman *et al.* 2004). None of the cervicals are co-ossified, unlike the co-ossified first three cervical vertebrae that occur in neoceratopsians (You & Dodson 2004).

Atlas. The proatlas is not preserved in any specimen. The atlas is well preserved and articulates with the occipital condyle in IVPP V18637 (Fig. 1A). The atlas consists of the atlantal intercentrum and paired atlantal neural arches. The atlantal intercentrum is robust and crescentic in cranial and caudal views (Fig. 1A, B). In cranial view, the surface is concave and smooth caudodorsally with a thin flange ventrally forming a shallow and wide fossa for accepting the occipital condyle (Fig. 1B). This fossa is deepest at the midline and becomes shallower laterally. The caudal surface is moderately convex (Fig. 1A). A small boss (diapophysis) is present on the ventrolateral region of each side of the atlantal intercentrum for articulation with a single-headed atlantal rib (Fig. 1A). A shallow transverse groove is present between the paired diapophyses on the caudoventral surface of the intercentrum, as also occurs in the basal neornithischian *Hexinlusaurus* and the ornithopod *Jeholosaurus*, but is unknown in other ceratopsians (He & Cai 1984; Han *et al.* 2012). Additionally, a small, oval bone is present between the occipital condyle and the atlantal intercentrum (Fig. 1A), which may represent a hypocentrum, as reported in *Protoceratops* (Brown & Schlaikjer 1940).

The paired neural arches articulate with the atlantal intercentrum dorsolaterally (Fig. 1A). Each arch forms an inverted 'L' shape, which consists of a horizontal ramus (dorsally) and a vertical ramus (ventrally). The horizontal ramus is dorsoventrally compressed, thin, and expanded craniocaudally to form the pre- and postzygapophyses, suggesting the presence of a proatlas. The paired horizontal rami do not contact each other at the midline. The postzygapophysis tapers caudally. A deep fossa is formed at the junction between the dorsal and vertical rami on the medial surface (Fig. 1A). The vertical ramus is robust with a subrectangular cross section. It is expanded where it articulates with the intercentrum and thins transversely towards the dorsal ramus, creating a subrectangular outline when viewed laterally.

Axis. The axis is preserved only in IVPP V18636. Unfortunately, the centrum is missing and only the neural spine is complete (Fig. 1E). In lateral view, the neural spine extends caudodorsally at an angle of about 30°. Rather than being laterally compressed, the axial neural spine forms a transverse plate, which is arched near the base and becomes more flattened distally. The neural spine extends to the distal end of the centrum of the third cervical vertebra, as in *Psittacosaurus* and neoceratopsians (e.g. *Protoceratops*) (Brown & Schlaikjer 1940; Averianov *et al.* 2006), whereas it appears to be short and

tall in *Chaoyangsaurus* (Zhao *et al.* 1999), *Hexinlusaurus* (He & Cai 1984), the basal ornithopod *Hypsilophodon* (Galton 1974) and *Haya* (Makovicky *et al.* 2011). A long axial neural spine is also seen in *Heterodontosaurus* (Santa Luca 1980), *Lesothosaurus* (Baron *et al.* 2017) and some basal ornithopods, including *Changchunsaurus* and *Jeholosaurus* (Butler *et al.* 2011; Han *et al.* 2012).

Cervical vertebrae 3–9. The cervicals are not fully prepared in IVPP V18636, and can only be seen in dorsal and lateral views (Figs 1, 2). Most of the centra and neural arches are still concealed in the matrix. The neural spines are small and short except for the somewhat elongated spine of cervical 9. In IVPP V18636, the neural spine of cervical 3 is concealed and its size is unknown, but it probably rudimentary, as in other ornithischians except *Heterodontosaurus* which has a prominent caudodorsally extending neural spine (Santa Luca 1980). The neural spine of cervical 4 is short, transversely narrow and tapers distally in lateral view, and its base is positioned between the postzygapophyses. Most of the other neural spines are damaged, but their cross sections reveal they were small with sub-triangular bases.

In IVPP V18636, the neural spine of cervical 9 is preserved. It is erect, extends caudodorsally, and has a wedge-shaped outline in lateral view (Fig. 1E). It is approximately one-third the length of the neural spine of the first dorsal vertebra.

The prezygapophyses and postzygapophyses are short and positioned at the same level. The articular surfaces of the postzygapophyses are broad and oval, and extend along the entire length of the zygapophyses. Additionally, they face caudolaterally, forming an angle of 45° to the horizontal. When viewed dorsally, the paired postzygapophyses form a right angle with each other. There is no trace of epipophyses, which occur in *Lesothosaurus* (Sereno 1991; Baron *et al.* 2017), *Heterodontosaurus* (Santa Luca 1980) and *Manidens* (Pol *et al.* 2011).

The diapophyses are well developed and located at the centre of the neural arch in lateral view. The diapophyses on the most cranial cervical are short and compressed dorsoventrally, whereas the diapophyses on the caudal cervicals become more robust and elongate with a sub-circular cross section.

Two well-preserved, isolated cervical vertebrae are present in IVPP V18684 (Fig. 1C, D). Both appear to be from the more caudal portion of the cervical series due to their sub-circular diapophyses. The centra are amphiplatyan, and are slightly taller than they are wide. The height of the centra slightly exceeds the length, as in other ceratopsians such as *Psittacosaurus* (Averianov *et al.* 2006). The parapophyses are stout oval processes, and are positioned on the craniodorsal margin of the centrum. The neural arch spans nearly the entire length of the centrum. The large neural canal is large at the base, narrows

dorsally, and is slightly shallower than the height of the centrum.

The post-axial cervical ribs are missing on the more cranial cervical vertebrae, but the more caudal ones are present in IVPP V14530 and IVPP V18636 (Fig. 1E). They are shorter but more robust than the first few dorsal ribs. The proximal ends of the cervical ribs have a short capitulum and a much long tuberculum. The capitulum is short, wide and subrectangular in outline, whereas the

tuberculum is long and narrow. The rib shafts are plate like, craniocaudally compressed and taper distally to blunt ends. The caudal surface is smooth and concave, and the ribs curve gently ventromedially. The preserved cervical ribs lengthen gradually down the series but remain notably shorter than the first dorsal rib (Fig. 1E).

Dorsal vertebrae. The dorsal vertebrae are well preserved in IVPP V18636 and IVPP V18684 (Fig. 2).
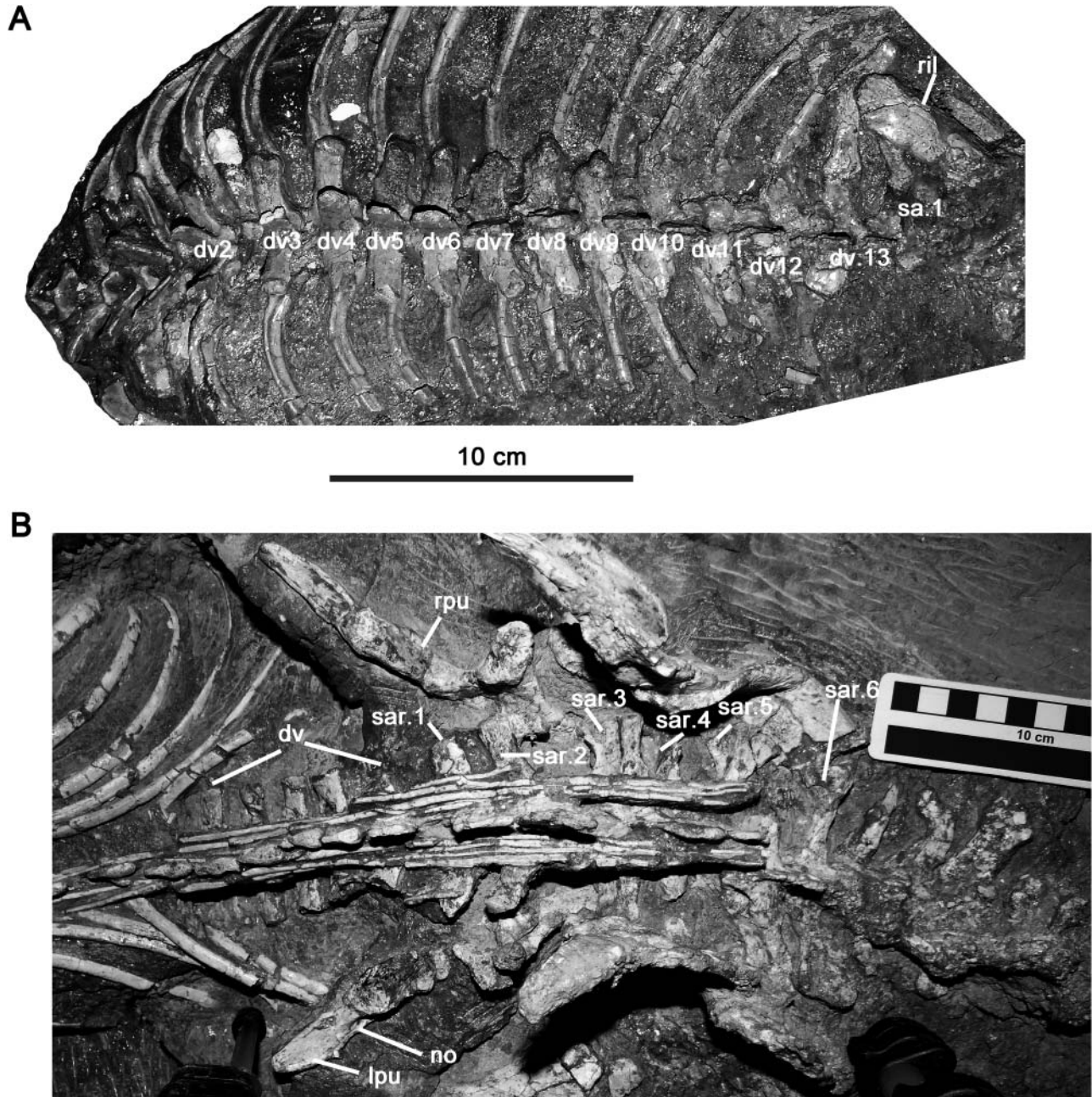
Figure 2. Photographs of dorsal and sacral vertebrae of *Yinlong downsi* in dorsal view. **A,** IVPP V18636, dorsal vertebrae in dorsal view. **B,** IVPP V18684, articulated dorsal vertebrae, sacral vertebrae and pelvic girdles in dorsal view. Abbreviations: ax, axis; cr, cervical rib; cv, cervical vertebra; dr, dorsal rib; dv, dorsal vertebrate; lpu, left pubis; no, notch; ns, neural spine; poz, postzygapophysis; ril, right ilium; rpu, right pubis; sa, sacral vertebra.

Unfortunately, most of the centra and neural arches are still covered in matrix. This does not allow us to identify the first dorsal vertebra based on the position of the parapophysis (Sereno 1987). However, the first dorsal vertebra can be recognized based on the morphology of the neural spine and ribs. The short neural spine of the last cervical is wedge shaped and directed caudodorsally, whereas the neural spine of the first dorsal vertebra is tall, subrectangular and relatively erect. Additionally, the first dorsal rib is much longer but more slender than the last cervical rib (Fig. 2).

There are 13 articulated dorsal vertebrae in IVPP V18636 (Fig. 2A), which also occurs in some *Psittacosaurus* species (Sereno 1990) and the ceratopsid *Anchiceratops* (Mallon & Holmes 2010), whereas 14 dorsals are preserved in *Auroraceratops* (Morschhauser 2012) and *Psittacosaurus sibiricus* (Averianov *et al.* 2006) and 12 dorsals are seen in most basal neoceratopsians, such as *Protoceratops* and *Leptoceratops* (Brown & Schlaikjer 1940, 1942). In other basal ornithischians, Heterodontosaurids usually possess 12 vertebrae (Sereno 2012), and ornithopods usually have no fewer than 15 vertebrae (e.g. *Jeholosaurus* and *Hypsilophodon*).

Disarticulated dorsal vertebrae in IVPP V14530 show that the centra are amphyplatyan. The centra of the middle and caudal dorsal vertebrae can be seen in lateral and dorsal view and show that centrum width is about equal to height, but both are less than their length. The lateral surfaces are craniocaudally concave with several small neurovascular foramina. The neural canal is small, and transversely wider than high.

The transverse processes are long, robust and dorsoventrally compressed. In dorsal view, they have a subrectangular outline and extend almost directly laterally from the neural arch. The dorsal surface is smooth and flattened, whereas the ventral surface expands ventrally to its base. The diapophysis is located at the distal end of the transverse process. The parapophysis is located below the transverse process in the first few dorsal vertebrae, but moves out along the transverse processes until it meets the diapophysis by the eighth dorsal vertebra. The diapophyses are completely fused together in the last dorsal vertebra. The pre- and postzygapophyses lie nearly at the same level. The articular surfaces are oval and smooth, forming an angle of 45° with the horizontal. The articulation between zygapophyses is unlike that of pachycephalosaurs and *Auroraceratops* which have rugose surfaces and a tongue-and-groove articulation (Maryańska & Osmólska 1974; Morschhauser 2012).

The neural spines are transversely compressed, laterally flattened and subrectangular in lateral view. Spine height is twice its axial length, as in *Psittacosaurus* and basal neoceratopsians (Sereno 1987; You & Dodson 2004), whereas in basal ornithischians *Lesothosaurus* (Baron *et al.* 2017), *Heterodontosaurus* (Santa Luca 1980),

Hexinlusaurus (He & Cai 1984), basal ornithopods *Jeholosaurus* (Han *et al.* 2012), *Hypsilophodon* (Galton 1974) and *Haya* (Makovicky *et al.* 2011), neural spine height is less than 1.5 of the width. The neural spines of the first dorsal vertebrae are narrow craniocaudally and thin transversely, and become wider and thicker caudally (Fig. 2). The neural spines of the more caudal dorsal vertebrae have thin cranial edges and thick caudal edges, giving them a wedge-shaped cross section.

The dorsal ribs are well preserved in IVPP V18636. The first four ribs become progressively longer; the fourth rib is the longest in the body. The dorsal ribs then shorten gradually to the 15th rib. Most of the dorsal ribs are double headed, although the tuberculum and capitulum move closer together down the series; only the last three are single headed. The first few ribs are robust, curve ventrally, and taper to their distal ends. Well-developed grooves are present along the caudal surfaces of the first six dorsal ribs, whereas the cranial surfaces are convex, forming a semilunar cross section. The caudal ribs are relatively slender and less curved with a sub-circular cross section.

Sacral vertebrae. Sacral vertebrae are preserved in many specimens, but no specimen preserves an articulated series. The sacrum consists of six sacral vertebrae based on IVPP V18682 and IVPP V18684 (Fig. 2B).

Six sacral vertebrae are also known in *Psittacosaurus* (Averianov *et al.* 2006), some basal neoceratopsians, such as *Archaeoceratops* (You & Dodson 2003), pachycephalosaurs (Maryańska *et al.* 2004), *Heterodontosaurus* (Santa Luca 1980) and basal ornithopods (e.g. *Jeholosaurus*, Han *et al.* 2012), whereas in most neoceratopsians, such as *Auroraceratops* (eight) and *Protoceratops* (eight), there are more than six sacrals (Brown & Schlaikjer 1940; Morschhauser 2012). Five sacrals are seen in some basal ornithischians, such as *Lesothosaurus* (Sereno 1991), *Agilisaurus* (Peng 1992), *Hexinlusaurus* (He & Cai 1984) and *Scutellosaurus* (Norman *et al.* 2004). Four sacrals occur in *Scelidosaurus* (NHMUK R6704; Norman *et al.* 2004), and the pachycephalosaur *Geyocephale* (Perle *et al.* 1982).

The identification of sacrals is mainly based on the neural spine morphology and presence of sacral ribs in IVPP V18684 (Fig. 2B). In dorsal view, the neural spines are craniocaudally long, shorter than the height of the centra, and contact each other (Fig. 3). Additionally, the distal end of the neural spine has a subrectangular cross section, unlike the caudal dorsal vertebrae where the spines are thickened caudally and have subtriangular cross sections. The first two sacral transverse processes are subrectangular and extend craniolaterally. They still bear independent ribs (Fig. 2), as also seen in *Auroraceratops* (Morschhauser 2012). The sacral ribs fuse to the sacral transverse process from the third through to the sixth sacral. They are hour-glass shaped in lateral view. Sacral ribs 3 and 4

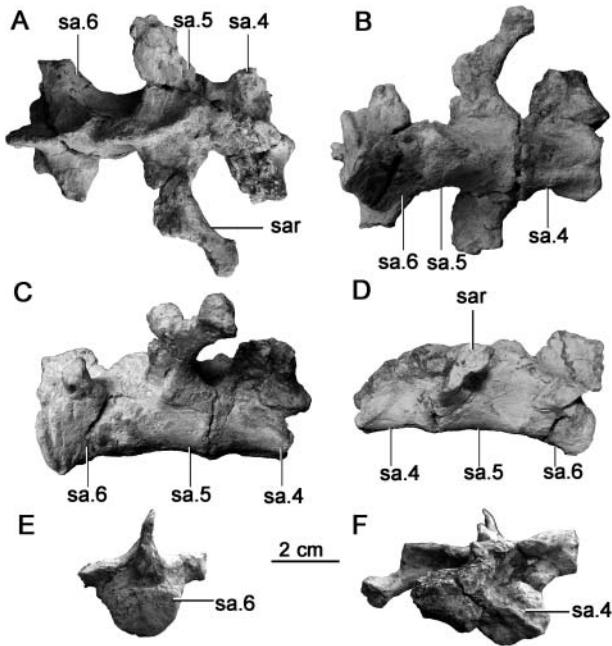**Figure 3.** Photographs of sacral vertebrae of *Yinlong downsi*, IVPP V18637. **A,** dorsal view; **B,** ventral view; **C,** right lateral view; **D,** left lateral view; **E,** caudal view; **F,** cranial view. Abbreviations: sa, sacral vertebra; sar, sacral rib.

extend laterally while sacral ribs 5 and 6 extend caudolaterally. The caudal sacral ribs are longer than the cranial ones, as in other marginocephalians, such as *Archaeoceratops*, *Auroraceratops* (You & Dodson 2003; Morschhauser 2012), and pachycephalosaurs (Maryańska & Osmólska 1974). However, in *Psittacosaurus*, the sacral ribs are all subequal in length.

IVPP V18637 has three articulated sacral vertebrae (Fig. 3). The sacral centra are uniformly wider than they are high, although both these dimensions are exceeded by the length of the centra. The sacral rib of the third preserved vertebra articulates only with the centrum of that vertebra, indicating that this is the last, or sixth, sacral and strongly suggests that these are sacrals 4–6 (Galton 1974, figs 23, 24). The cranial and caudal centra faces are amphiplatyan. In cranial view, the centra are transversely expanded and dorsoventrally compressed with semi-lunar cross sections (Fig. 3E). The first preserved sacral (sacral 4) bears a shallow longitudinal groove at the ventral midline, whereas the ventral surfaces of the other two centra are rounded. In lateral view, the ventral margins of the sacral centra are slightly concave.

In sacral 4, only the centrum and right sacral rib are preserved. This sacral rib is robust and dorsoventrally compressed. The proximal end forms two articular surfaces. The cranial articular surface is small and oval shaped and faces craniomedially, most likely for articulation with the centrum of sacral 3. The caudal articular surface is much larger and articulates with most of the sacral 4 centrum.

Sacral 5 is well preserved and bears two partial sacral ribs. Its centrum is not fused to that of sacral 4. Most of the sacral rib articulates with the centrum of sacral five and only a small part articulates with the caudal margin of the sacral 4 centrum. The fifth sacral rib is deep dorsoventrally and narrow craniocaudally, and constricts dorsoventrally between its contacts with the centrum and ilium. It articulates with the diapophysis dorsally and the centrum ventrally. Deep fossae are present on the cranial and caudal surfaces of the rib (Fig. 3D). The dorsal edge of the sacral rib is slightly convex, and the distal end tapers slightly. The pre- and postzygapophyses are small and transversely narrow. The neural spine is thickened, long, and located above the neural arch and postzygapophyses.

The centrum of sacral 6 is completely fused to that of sacral 5. In lateral view, the caudal end of the centrum curves ventrally. The neural canal is elliptical with the long axis oriented mediolaterally. The neural spine is long craniocaudally with a subrectangular outline in lateral view. The sixth sacral rib is born wholly on the centrum but only its proximal portion is preserved. The preserved sacral rib is short dorsoventrally, craniocaudally expanded with an oval cross section, and is oriented slightly caudally.

Caudal vertebrae. The complete number of caudal vertebrae is uncertain. However, in IVPP V18685, 40 well-preserved caudals are present, and only a few may be missing (Fig. 4D; Supplemental Appendix 1). The first 17 articulated caudals are preserved in IVPP V18677. Sixteen caudal vertebrae are preserved in the holotype IVPP V14530 and the first six are in articulation (Fig. 4).

The caudal centra are amphyplatyan. They are taller than wide, but both dimensions are exceeded by the central length. Caudally, the centra become transversely narrower, as in *Psittacosaurus* (You & Dodson 2004), whereas in neoceratopsians such as *Protoceratops* and *Leptoceratops* the centra are deeper and wider than they are long in the more cranial region (Brown & Schlaikjer 1940). In *Auroraceratops*, the cranial and middle caudal centra have equal length and height, and the length exceeds the height only at the distal end (Morschhauser 2012).

In ventral view, the chevron facets are oval in outline and located on the cranial and caudal edge of the centrum. The caudal facets are more developed than the cranial facets, as chevrons are born primarily on the preceding vertebra. The position of the first chevron is unknown. The transverse processes are long, craniocaudally narrow and dorsoventrally compressed. They are similar in length to the neural spines but narrower craniocaudally than the latter. In IVPP 14530 the transverse processes are not fused to the neural arch. The facet for the transverse process indicates they were born primarily on the neural arch, but that their ventral aspect articulates with the centrum. They
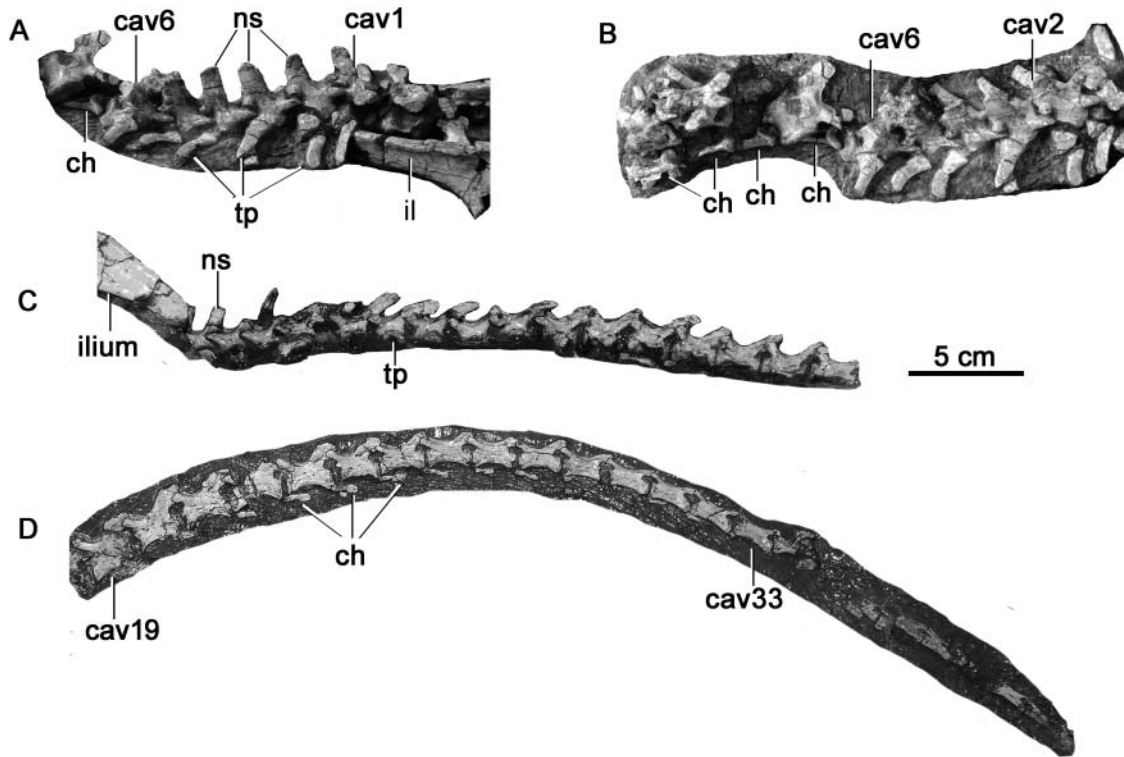
Figure 4. Photographs of caudal vertebrae of *Yinlong downsi* in lateral view. **A, B,** IVPP V14530, cranial part in **A,** lateral view; **B,** dorsal view. **C,** IVPP V18677, cranial part in left lateral view. **D,** IVPP V18685, caudal region in left lateral view. Abbreviations: cav, caudal vertebra; ch, chevron; ns, neural spine; tp, transverse processes.

extend caudolaterally and form an angle of 45° with the long axis of the caudal vertebrae. In IVPP V14530 and IVPP V18637, the distal ends of the transverse processes on the first few caudals curve cranially, but this is not seen in other specimens. The transverse processes are reduced in length caudally and completely disappeared after caudal 20 (Fig. 4).

In lateral view, the pre- and postzygapophyses are nearly at the same level. The prezygapophyses are well developed with a sub-circular outline and are oriented 45° to the horizontal, whereas the postzygapophyses are small and narrow. The prezygapophyses extend cranially over the preceding centrum in the first few caudals; in the middle and caudalmost caudal vertebrae the prezygapophyses shorten and no longer extend beyond the cranial limit of their centra. Deep fossae lie between prezygapophyses and the neural spine in the first four caudals (IVPP V18677).

The neural spines of the first few caudals are mediolaterally slender, and rectangular in lateral view with sharp edges on both cranial and caudal sides. The height of the first few neural spines are less than 1.5 times the height of the centra, unlike in most neoceratopsians (e.g. *Protoceratops* and leptoceratopsids) where the neural spines are more than twice the height of the centra. The neural spines are positioned on the caudal half of the centra and above

and between the postzygapophyses. They extend caudodorsally at an angle of approximately 60° from horizontal (IVPP 18677) and terminate in a sub-rectangular distal end. Caudally, the neural spines shorten and recline further to an angle of about 40°. In IVPP V18685, the neural spines disappear after caudal 30.

Chevrons. Many of the chevrons are well preserved in IVPP V14530 and IVPP V18684. In IVPP V14530, four disarticulated, well-preserved chevrons are present (Fig. 4). In caudal view, the chevron is Y-shaped. The expanded proximal end forms two articular processes for articulating with the centrum. These processes form the lateral margins of the haemal canal and merge distally to form the chevron blade. Each articular process is divided into a craniodorsal and a caudodorsal facing articular facet. The craniodorsal articular surface is smaller than the caudodorsal facet. The chevron blades are mediolaterally compressed and often damaged at the distal end. In IVPP V18684, the distal ends of 19 to 26 are craniocaudally expanded, as in *Psittacosaurus*, and the neoceratopsians *Auroraceratops* and *Koreaceratops* (Averianov *et al.* 2006; Lee *et al.* 2011; Morschhauser 2012). However, the preserved chevrons of *Yinlong* are shorter than the length of the associated centra, whereas in

Auroraceratops the chevrons at the same positions are about the same length as their centra, and in *Koreaceratops* the chevrons (18 to 25) are twice the length of their associated centra (Lee *et al*. 2011). The heterodontosaurid *Tianyulong* also bears craniocaudally expanded chevron blades, but is has a horizontal ventral margin and subtriangular outline in lateral view (Sereno 2012).

Ossified tendons. Ossified tendons are well preserved in IVPP V14530, IVPP V18682 and IVPP V18684 (Fig. 2; Supplemental Appendix 1). They are elongate, transversely narrow and dorsoventrally expanded with an oval cross section. About five ossified tendons are gathered together in parallel along the lateral side of the neural spines of all the preserved dorsal and sacral vertebrae but do not extend into the caudal series. There is no trace of ossified tendons along the tail, which have been reported in many ornithopods (e.g. *Hypsilophodon*), the heterodontosaurid *Tianyulong* (Sereno 2012) and pachycephalosaurs (Maryańska & Osmólska 1974).

Appendicular skeleton

Scapula. Both scapulae are well preserved in IVPP V14530, IVPP V18684 and IVPP V18678, and are long and gracile (Fig. 5). The scapula shaft is mediolaterally compressed and bowed laterally to conform to the contours of the ribcage. It has a suboval cross section proximally.

Distally the scapula expands craniocaudally, as in most basal ornithischians, but unlike the conditions of *Eocursor* and *Stenopelix* where the scapular blades are only weakly expanded (Butler & Sullivan 2009; Butler 2010). Both the lateral and medial surfaces become flattened distally.

The dorsal end of the scapula is about twice the craniocaudal breadth of the narrowest part of the scapular neck. It is asymmetrical and thins mediolaterally from the neck to the distal end. The scapular blade is slightly concave along the cranial margin and straight along its caudal margin when viewed laterally. However, the degree of concavity is larger in small individuals, which may represent ontogenetic variation, as in *Protoceratops* (Brown & Schlaikjer 1940).

Ventrally, the scapula expands craniocaudally towards the glenoid and thickens mediolaterally to the coracoid articulation. The lateral surface of the articular end is smooth and nearly flat. The glenoid fossa is thick transversely with an oval, concave articular surface that faces cranioventrally. The coracoid articulation is wide and much more extensive than the glenoid fossa.

In overall morphology, the scapula is long and narrow, as in other ceratopsians, such as *Psittacosaurus* (Sereno 1987), *Auroraceratops* (Morschhauser 2012) and *Protoceratops* (Brown & Schlaikjer 1940). In *Heterodontosaurus*, the scapula is even more elongate, whereas in basal ornithopods, such as *Hypsilophodon*, the scapula is relatively wider (Galton 1974).
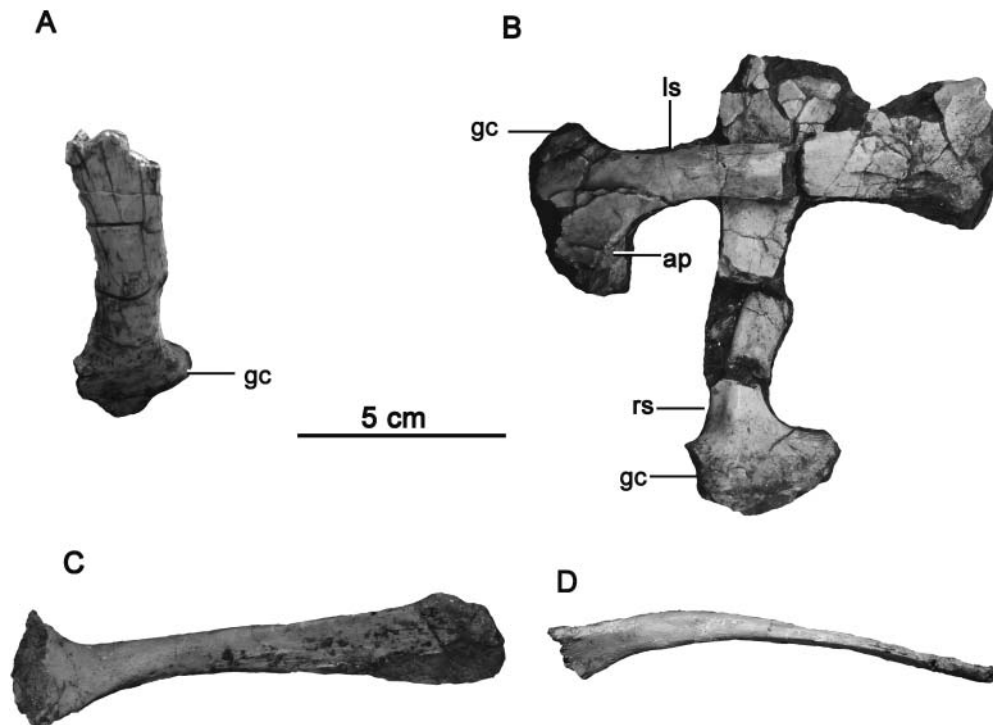

Figure 5. Photographs of scapulae of *Yinlong downsi*. **A,** IVPP V14530, left scapula in lateral view; **B,** IVPP V18678, right scapula in lateral view, and left scapula in medial view. **C, D,** IVPP V18684, right scapula in **C,** medial view and **D,** cranial view. Abbreviations: ap, acromial process; gc, glenoid cavity; ls, left scapula; rs, right scapula.

Coracoid. The coracoid is preserved in IVPP V18686. Unfortunately, it is seriously damaged and only its outline in medial view can be seen. It articulates with, but is not fused to, the scapula. It has a prominent coracoid process, and the medial surface is slightly concave. The coracoid foramen cannot be discerned.

Forelimb.

Humerus. The humerus is present in IVPP V14530 and IVPP V18684. The well-preserved but damaged humerus of IVPP V18679 is fully prepared (Fig. 6). The humerus is more slender and shorter than the scapula in IVPP V18684 (the ratio equals 0.91), as in most basal ornithischians except *Hexinlusaurus* (He & Cai 1984) and *Agilisaurus* (Peng 1992) which have relatively long humeri. The ratio of humerus to femur is about 0.6 in IVPP V18684, as in most ornithischians, whereas *Agilisaurus* (0.48, Peng 1992) and the pachycephalosaur *Wannanosaurus* have a humerus to femur ratio of less than 0.5 (Butler & Zhao 2009). The proximal end curves medially and has a distinctly concave cranial surface. The proximal margin of the humerus is convex, thickened craniocaudally, and has a rugose surface. A ball-like humeral head extends caudally from the proximal margin at its mid-point. A prominent longitudinal ridge extends from the humeral head down the caudal surface of the proximal humerus (Fig. 6C, D). The distinct and discrete deltopectoral crest is well developed and extends half way down the lateral margin of the humerus (Fig. 6A, B). The lateral margin of the deltopectoral crest is sub-round in outline, and curves craniolaterally (Fig. 6B, D), as in most basal ornithischians, whereas in pachycephalosaurs *Stegoceras* and *Wannanosaurus*, the deltopectoral crest is low and only slightly thickened (Maryańska *et al*. 2004; Butler &

Zhao 2009). The deltopectoral crest is thick at the base but thins to its distal margin. Most part of the caudal surface is flattened and forms a right angle with the humeral shaft may due to compression (Fig. 6C, D).

The cross section of the humerus below the deltopectoral crest is subcircular and slightly craniocaudally compressed. The humerus has an expanded distal end forming the medial and lateral condyles. The condylar width is slightly less than that of the proximal end. The medial condyle is broader mediolaterally and extends further ventrally than the lateral condyle, as also occurs in other ceratopsians, such as *Auroraceratops* (Morschhauser 2012), *Leptoceratops* (Brown 1914), and *Psittacosaurus* (Averianov *et al*. 2006), and the basal ornithischian *Lesothosaurus* (Baron *et al*. 2017). Distally a deep and transversely wide sulcus separates the two condyles on the cranial surface, whereas in caudal view only a shallow sulcus is present. In distal view, the lateral condyle is nearly round, and the medial condyle is sub-triangular.

Ulna. The ulna is well preserved in IVPP V14530 and IVPP V18677, and a complete ulna and radius are preserved in IVPP V18679. The ulna has a nearly straight shaft with a flat medial surface and an oval cross section (Fig. 7A, D). The ulnar shaft maintains a nearly uniform width for its entire length, expanding craniocaudally and mediolaterally only at its proximal end. Proximally, the robust olecranon process occupies approximately one half of the craniocaudally expanded proximal ulna, and rises a short distance above the proximal articular surface (Fig. 7A, E). The proximal articular surface slopes cranioventrally and tapers cranially. The olecranon process also expands mediolaterally to twice the width of the more cranial articular surface (Fig. 7E). A thick ridge extends from
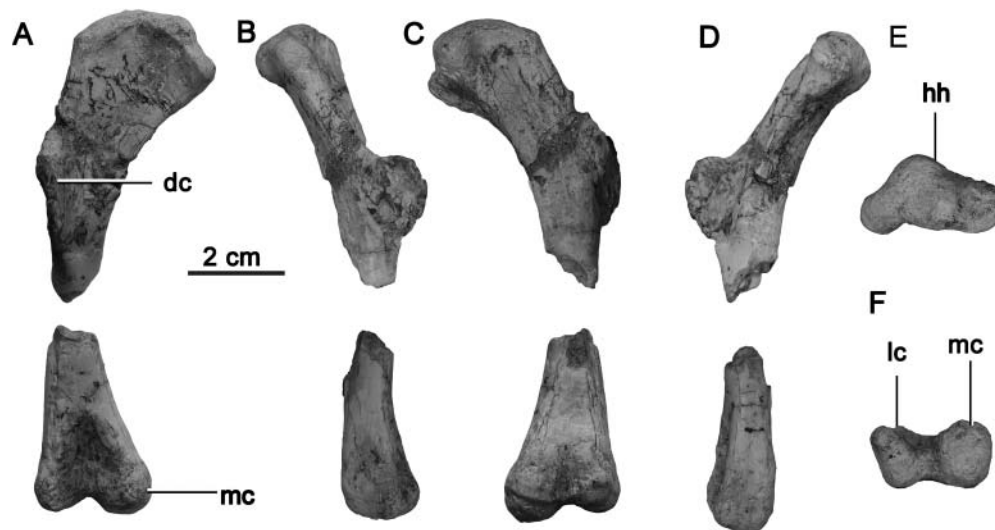

Figure 6. Photographs of humerus of *Yinlong downsi*, IVPP V18679. **A,** craniomedial view; **B,** dorsal view; **C,** lateral view; **D,** cranial view; **E,** dorsal view of the proximal end; **F,** ventral view of the distal end. Abbreviations: dc, deltopectoral crest; hh, humeral head; lc, lateral condyle; mc, medial condyle.
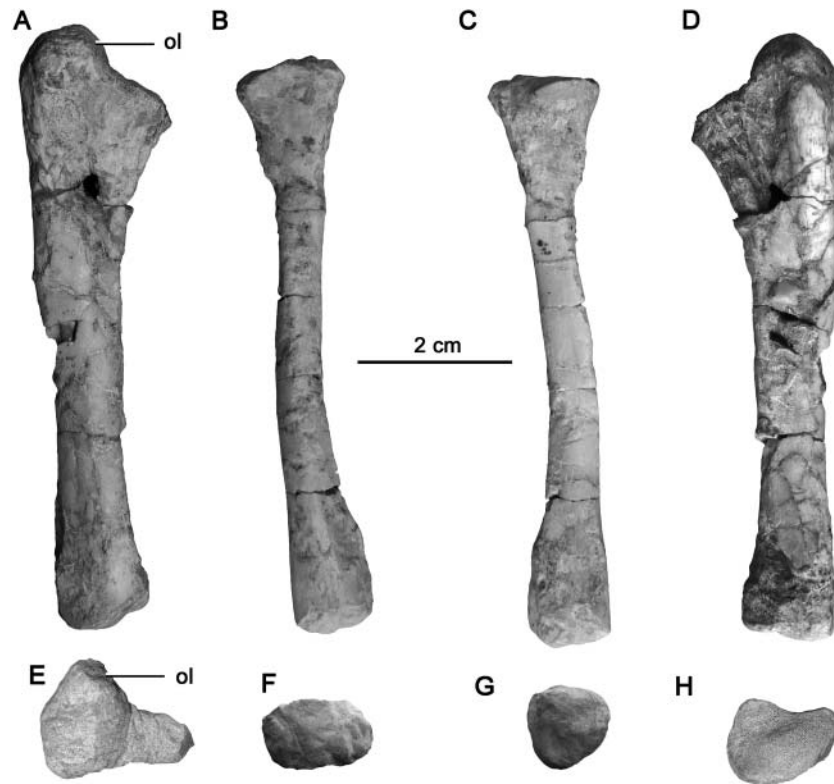
Figure 7. Photographs of the ulna and radius of *Yinlong downsi*, IVPP V18679. **A,** cranial view of the left ulna; **B,** cranial view of the left radius; **C,** caudal view of the left radius; **D,** caudal view of the left ulna; **E,** dorsal view of the left ulna; **F,** ventral view of the left ulna; **G,** dorsal view of the left radius; **H,** ventral view of the left radius. Abbreviation: ol, olecranon process.

the olecranon process distally along the caudolateral surface of the proximal half of the shaft. The distal articular surface is semilunar in cross section with a slightly indented lateral margin (Fig. 7H). The ulna is about 70% the length of the humerus (IVPP V18684).

Radius. The radius is slender and straight with a subtriangular cross section at midshaft (Fig. 7B, C). The proximal end is mediolaterally expanded and is oval in proximal view (Fig. 7F). The proximal articular surface is rugose and slightly convex. The distal end expands slightly in all directions and is sub-rounded in distal view with a rugose, slightly convex articular surface (Fig. 7G). The narrowest part of the radial shaft is approximately half that of the ulnar shaft.

Carpus and manus. The manus is well preserved in IVPP V14530, IVPP V18685 and IVPP V18684, but a complete carpus is not known. In IVPP V14530, an irregular carpal is present between the ulna and metacarpal III, and it may be the intermedium. A large carpal with an elliptical cross section is present distal to the radius, and may be the radiale (Fig. 8A). A small pit pierces the centre of this latter element in cranial view, as also seen in *Psittacosaurus* (Sereno 1987), *Auroraceratops* (Morschhauser 2012) and *Leptoceratops* (Brown 1914). Additionally, a

large oval bone is present on the cranial surface of the radius that may represent a carpal but this cannot be confirmed (Fig. 8A). In IVPP V18685, a robust, subtriangular bone on the medial side of metacarpal IV may represent the ulnare (Fig. 8C).

The manus contains at least four metacarpals. A small bone that is located at the lateralmost side of metacarpal IV may represent metacarpal V, although it may also be part of the proximal end of metacarpal IV (Fig. 8B). Five metacarpals are known in the neoceratopsians *Auroraceratops*, *Protoceratops*, *Leptoceratops* and *Montanoceratops* (Brown & Schlaikjer 1940; Chinnery & Weishampel 1998; Morschhauser 2012), as well as in basal ornithischians such as *Heterodontosaurus* (Santa Luca 1980), *Lesothosaurus* (Baron *et al.* 2017) and *Hexinlusaurus* (He & Cai 1984). However, only four metacarpals are preserved in the most complete specimens of *Psittacosaurus* (Sereno 1990).

In the holotype IVPP 14530, metacarpals I to III are articulated, and metacarpal IV has been displaced and lies over metacarpals I and II (Fig. 8A). In IVPP V18685 and IVPP V18684, four metacarpals are preserved and articulated. In overall morphology, the metacarpals are small, short, and expanded at both their proximal and distal ends. The metacarpals are wider transversely than they
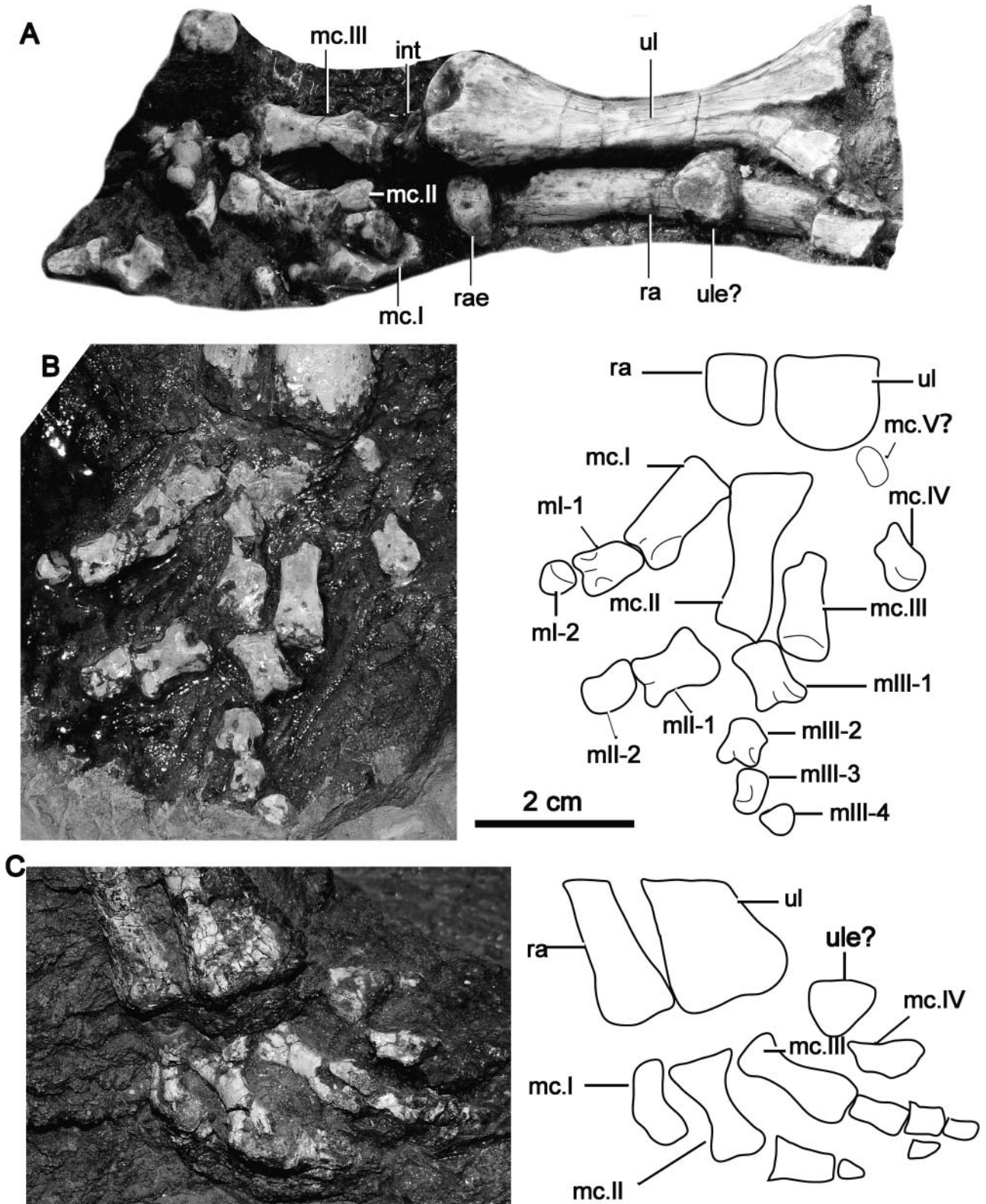
Figure 8. Photographs and line drawings of forelimbs of *Yinlong downsi*. **A,** IVPP V14530, dorsal view of the ulna, radius and manus. **B,** IVPP V18684, dorsal view of the manus. **C,** IVPP V18685, dorsal view of the manus. Abbreviations: int, intermedium carpal; mc, metacarpal; mI, II, III, manual digit I, II, III; ra, radius; rae, radiale; ul, ulna; ule, ulnare.

are dorsoventrally. Proximally, the mediolaterally expanded metacarpals contact one another but are not tightly appressed. Distally, the ginglymi are poorly developed and the condyles are not clearly separated. Ligament pits are well preserved on the sides of the condyles. Metacarpal I is the shortest, and is 70% the length of metacarpal II. Metacarpal III is the longest, and is 33% the length of the radius. Metacarpal IV is only known from the distal end. Based on its position in the articulated hand it appears to have been as long as metacarpal I, but more slender (Fig. 8B).

The phalangeal formula of *Yinlong* is 2-3-4-?-?. There are no preserved phalanges associated with metacarpal 4. The phalangeal formula is 2-3-4-1-0 in *Psittacosaurus* (Sereno 1990), 2-3-4-2-1 in *Auroraceratops* (Morschhauser 2012) and 2-3-4-3-1(or 2) in *Protoceratops*, *Leptoceratops* and *Montanoceratops* (Brown & Schlaikjer 1940; Chinnery & Weishampel 1998). The phalangeal count for the first three digits is stable in basal ornithischians (Sereno 2012), but it is increased in digits 4 and 5 in derived ceratopsians. However, *Heterodontosaurus* and the ornithopod *Hypsilophodon* all have three and two phalanges in digits 4 and 5, respectively (Galton 1974; Santa Luca 1980), which suggests that the reduced number of phalanges in ceratopsians represents a derived character.

The phalanges are well preserved and articulated in IVPP V18684. Digit 1 bears two phalanges. The first phalanx is half the length of the metacarpal, and the ungual is very small with a broad proximal articular surface and a tapered, rounded distal end. Digit 2 also preserves two phalanges, but is missing the ungual phalanx. Digit 3 bears four phalanges that rapidly decline in size and length distally. The fourth, ungual phalanx is short and rounded distally. The phalanges of digit 4 are missing in all specimens. All phalanges are similar in shape: they are short, transversely wide and dorsoventrally compressed. They are slightly expanded at both the proximal and distal ends. The proximal articular surface is concave, and the distal end forms distinct medial and lateral condyles separated by a sulcus. Ligament pits are present on the lateral surface of the condyles.

In overall morphology, the manus and phalanges are very similar to those of other ceratopsians, including *Psittacosaurus* and *Auroraceratops* (Averianov *et al.* 2006; Morschhauser 2012). This is unlike the condition seen in *Heterodontosaurus* (Norman *et al*. 2011) and basal ornithopods, such as *Hypsilophodon* (Galton 1974), which have relatively longer and more slender metacarpals and phalanges.

Ilium. The ilium is well preserved in IVPP V14530, IVPP V18637 and IVPP V18682 (Figs 9–11). The ilium is long and shallow, consisting of a central portion, a long and narrow preacetabular process and a long postacetabular process. The ilium from the base of the preacetabular process to the base of the postacetabular process has a length twice that of the depth over the acetabulum in all the preserved specimens, as in *Stenopelix* (Butler & Sullivan 2009) and *Abrictosaurus* (Sereno 2012). This is unlike other ceratopsians, pachycephalosaurs and ornithopods, which have a main body length less than 1.5 of the depth (Maryańska *et al*. 2004; You & Dodson 2004; Han *et al*. 2012).

In lateral view, the lateral surface of the ilium is smooth and slightly concave, and the entire dorsal margin is moderately convex upwards. The dorsal margin, particularly over the main body and postacetabular process, is thickened to the lateral side, accentuating the concave lateral surface. In dorsal view, the entire ilium is slightly sinuous and S-shaped (Fig. 10B): the preacetabular process extends craniolaterally, while the postacetabular process curves laterally at the basal and medially at its distal end, as in *Auroraceratops* (Morschhauser 2012). In *Archaeoceratops*, the postacetabular process extends only caudolaterally.

The preacetabular process is elongate, mediolaterally compressed, and gently curves ventrally to reach an angle of 30° from the horizontal at its cranial end. The preacetabular process is mediolaterally widest at the base, and narrows towards the distal end. The ventral margin of the distal end is expanded in IVPP V14530 and IVPP V18682 (Figs 9, 10), whereas it tapers in IVPP V18637 (Fig. 11). However, the distal end in the latter specimen is poorly preserved. The medial surface of the distal preacetabular process bears a series of craniocaudally oriented ridges (Fig. 9C). The expansion of the distal end of the preacetabular process is similar to that of basal neoceratopsians, such as *Liaoceratops* (IVPP V17910, FH pers. obs.), *Archaeoceratops* (You & Dodson 2003) and *Auroraceratops* (Morschhauser 2012). The distal end of the preacetabular process is also expanded in *Stenopelix* (Butler & Sullivan 2009) and pachycephalosaurs, such as *Homalocephale* (Maryańska & Osmólska 1974). However, in pachycephalosaurs the expansion occurs transversely along the dorsal margin, unlike that of ceratopsians. A ridge is present along the ventromedial surface of the preacetabular process that extends almost horizontally from the base of the process to the dorsal margin of the distal end.

The postacetabular process is deep at the base, and tapers caudally. It is equal to (IVPP V18637) or slightly shorter (IVPP V14530 and IVPP V18682) than the preacetabular process, as in other ceratopsians and pachycephalosaurs (You & Dodson 2004; Maryańska *et al*. 2004), but unlike the basal ornithischians *Lesothosaurus* (Baron *et al*. 2017), *Hexinlusaurus* (He & Cai 1984), *Agilisaurus* (Peng 1992) and *Heterodontosaurus* (Santa Luca 1980) and basal ornithopods *Jeholosaurus* (Han *et al*. 2012) and *Hypsilophodon* (Galton 1974), where the postacetabular processes are shorter and deeper. The dorsal edge of the
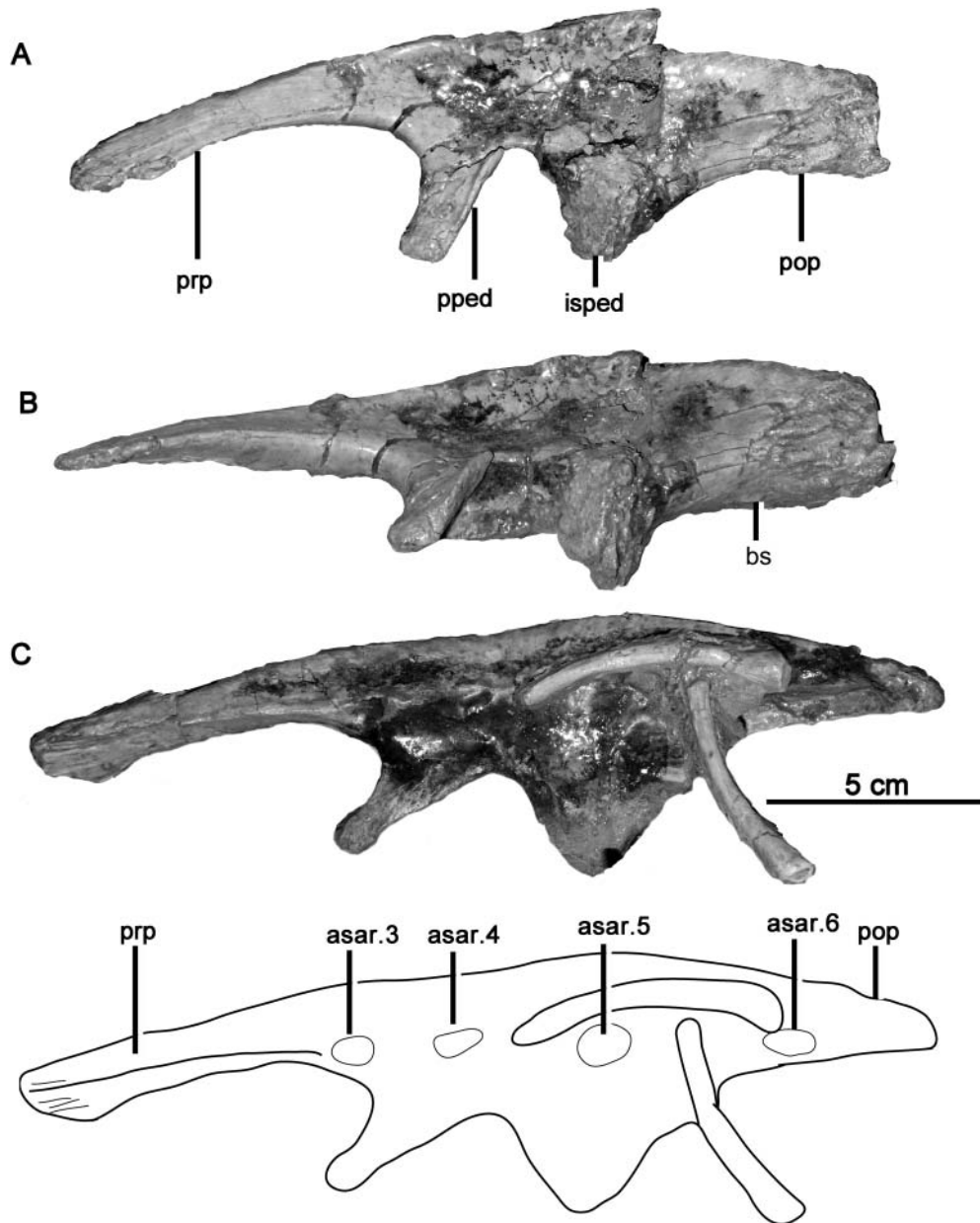
Figure 9. Photographs and line drawing of the ilia of *Yinlong downsi*, IVPP V18682. **A,** left ilium in lateral view; **B,** left ilium in ventral view; **C,** right ilium in medial view. Abbreviations: bs, brevis shelf; isped, ischiac peduncle; pop, postacetabular process; pped, pubic peduncle; prp, preacetabular process; sar, articulation for sacral rib.

postacetabular process curves gently downwards to its distal end while the ventral edge is nearly straight. In IVPP V18682 and IVPP V14530, the distal end of the postacetabular process tapers to a sharp end (Figs 9C, 10B), whereas in the large specimen IVPP V18637 it is blunt (Fig. 11A). This distinction may represent an ontogenetic or individual variation. A tapered distal postacetabular process is also seen in *Stenopelix* (Butler & Sullivan 2009). The postacetabular process is thick transversely with a subtriangular cross section due to its broad ventral margin that forms a flat, narrow brevis shelf (Fig. 9B).

However, it does not form a medial brevis fossa. The absence of a brevis fossa is also seen in other ceratopsians, such as *Psittacosaurus* (Sereno 1987) and *Archaeoceratops* (You & Dodson 2003). In pachycephalosaurs the ventral edge is not expanded (Maryańska & Osmólska 1974).

The acetabulum narrows dorsally so that it is subtriangular in lateral view. It is notably taller than it is craniocaudally wide. There is no supraacetabular shelf. The long and slender pubic peduncle extends cranioventrally and is sub-triangular in cross section for most of its length.
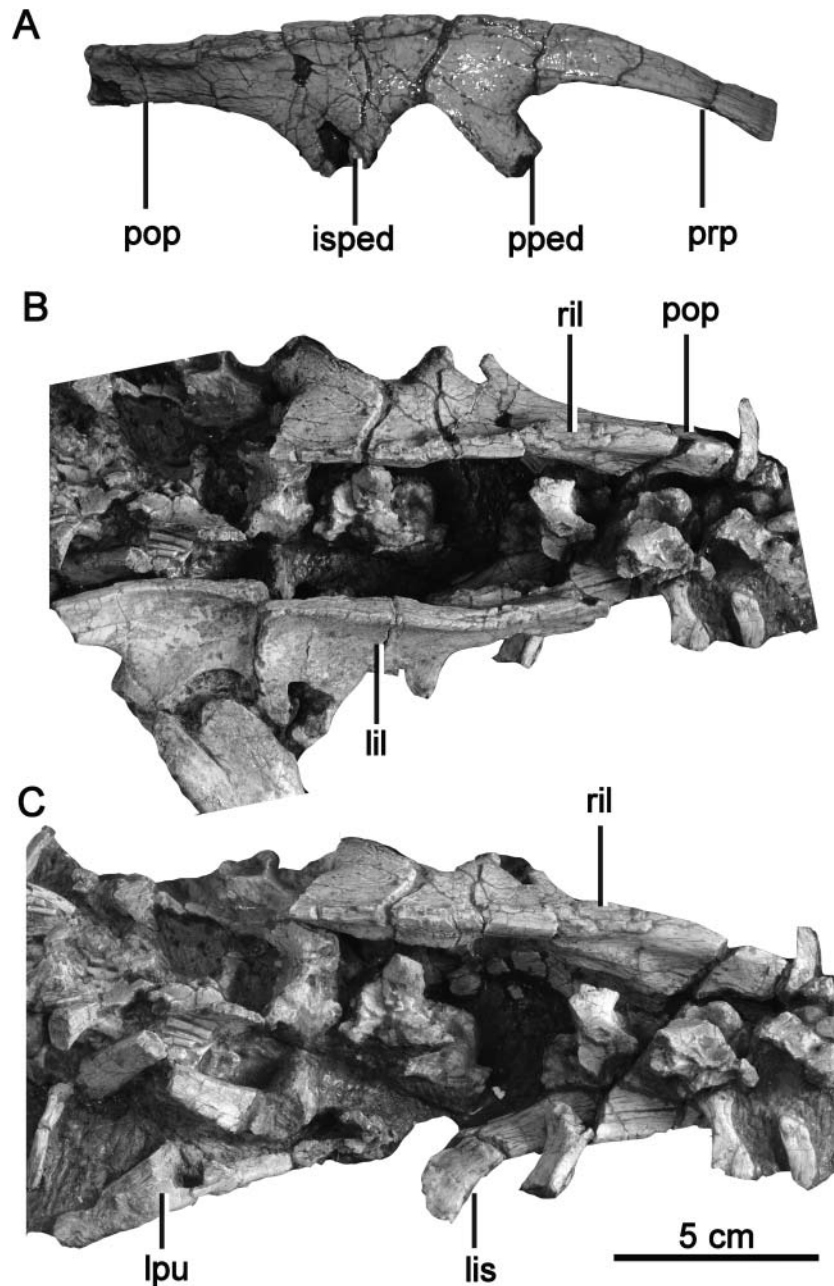
Figure 10. Photographs of the pelvic girdle of *Yinlong downsi*, IVPP V14530. **A,** ilium in lateral view; **B,** ilia in dorsal view; **C,** pelvic girdle with left ilium removed in dorsal view. Abbreviations: isped, ischiac peduncle; lil, left ilium; lis, left ischium; lpu, left pubis; pop, postacetabular process; pped, pubic peduncle; prp, preacetabular process; ril, right ilium.

It is transversely expanded to support a broad acetabular surface that faces caudomedially. Distally, the pubic peduncle ends in a slightly convex surface that articulated with the pubis.

The ischial peduncle is robust and triangular in lateral view. It extends ventrally to the same level as the pubic peduncle. The articular surface is slightly convex, as in the basal marginocephalian *Stenopelix* (Butler & Sullivan 2009), whereas it is usually strongly convex in other

ceratopsians, such as *Archaeoceratops* (IVPP V11115), pachycephalosaurs such as *Homalocephale* (Maryańska & Osmólska 1974) and ornithopods such as *Jeholosaurus* (Han *et al.* 2012). The caudal margin of the ischial peduncle is oriented caudodorsally to merge smoothly into the base of the postacetabular process. In the basal ornithopod *Jeholosaurus* the caudal edge of the ischial peduncle forms a right angle with the postacetabular process. In IVPP V18682 the ilium is exposed in medial view. Four
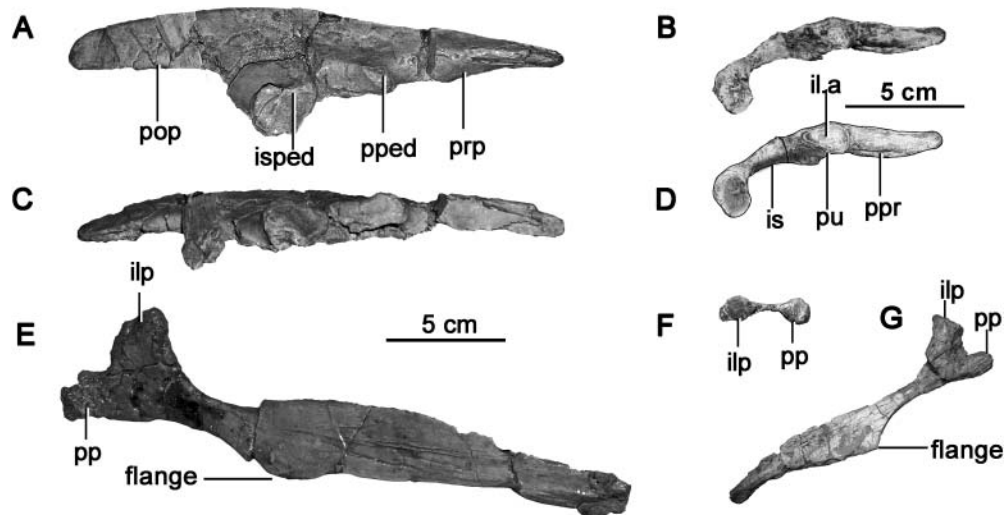
Figure 11. Photographs of ilia and ischia of *Yinlong downsi*. **A, C, E,** IVPP V18637; **A,** left ilium in lateral view; **C,** left ilium in ventral view; **E,** right ischium in dorsal view. **B, D,** IVPP V18684, photograph and outline drawing of articulated ischium and pubis in rostrodorsal view. **F, G,** IVPP V18679; **F,** left ischium in cranial view; **G,** left ilium in dorsal view. Abbreviations: il.a, articulation for ilium; ilp, iliac peduncle; is, ischium; isped, ischiac peduncle; no, notch; pop, postacetabular process; pp, pubic peduncle; pped, pubic peduncle; ppr, prepubic process; prp, preacetabular process; pu, pubis.

shallow fossae are shown at the midline for articulating with the sacral ribs (Fig. 9C). However, the articulation with the sacral rib is obscured by the overlying ilium. Based on *Auroraceratops* (Morschhauser 2012), the small and sub-circular cranial two fossae may articulate with sacral ribs 3 and 4. The third fossa is shallow and relatively large for articulating with sacral rib 5. The fourth fossa is present near the ventral margin of the postacetabular process, and may represent a facet for sacral rib 6.

In overall morphology, the ilium is similar to other basal ceratopsians. Its general outline and proportions of the pre- and post-acetabular processes fit a general pattern also seen in *Psittacosaurus* (Averianov *et al.* 2006), *Archaeoceratops* (You & Dodson 2003) and *Auroraceratops* (Morschhauser 2012). It differs from the ilia of pachycephalosaurs in which the dorsal margins are transversely expanded (Maryańska & Osmólska 1974), and from small basal ornithischians (e.g. *Hexinlusaurus*; He & Cai 1984), where the ilium usually has a thin dorsal edge and a postacetabular process that is shorter than the preacetabular processes.

Ischium. The right ischium of IVPP V18637 and the left ischium of IVPP V18679 are well preserved but only visible in medial view (Fig. 11E–G). The ischium is long, robust and lacks an obturator process.

The proximal end is divided into a slender pubic process and a relatively wide iliac process. They are relatively equal in length and both are mediolaterally compressed. The pubic process has a sub-circular cross section and expands mediolaterally to the distal articular facet. The surface of the pubic facet is flat. The iliac process is

subrectangular and also expands mediolaterally to the iliac articulation. In articular view the facet is broad cranially and narrows caudally. The angle between the pubic and iliac processes is approximately 120°. The acetabular margin is thin in the small individual IVPP V18679 but thick in the larger specimens IVPP V18679 and IVPP V18637. This may be due to ontogenetic variation.

The ischial shaft is mediolaterally narrow and plate-like. The lateral surface of the ischial blade is slightly convex while the medial surface is flat. It constricts to a narrow neck distal to the pubic and iliac processes, then expands, particularly ventrally, into a dorsoventrally deep blade that then tapers slightly distally. The ischial shaft is deepest where the ventral expansion forms a flange that marks the proximal contact between contralateral ischia (Fig. 11E). This feature is also seen in the marginocephalian *Stenopelix* where it has been considered an autapomorphy (Butler & Sullivan 2009). The flange in the ischial midshaft also occurs in the basal ornithischian *Laquintasaura*, but the latter is much more prominent (Barrett *et al.* 2014). This flange-like 'obturator process' is unlike the tab-shaped obturator process that is present in the large basal ornithischian *Lesothosaurus* (Butler 2005; Baron *et al.* 2017) and in ornithopods (e.g. *Hypsilophodon*; Galton 1974). Obturator processes are absent in heterodontosaurids (Sereno 2012), basal thyreophorans (Norman *et al.* 2004), ceratopsians (You & Dodson 2004) and pachycephalosaurs (Maryańska & Osmólska 1974). The absence of an obturator process was suggested to be an ontogenetic feature in *Lesothosaurus*, but both the young and adult *Yinlong* specimens lack the

obturator process, which suggests that this feature is not ontogenetically related in *Yinlong*. Distally, the entire ischial shaft curves slightly ventrally and expands medio-laterally at the distal end to terminate in a sub-rectangular cross section.

In overall morphology, the ischium can be distinguished from other basal ornithischians by a shaft that is deepest at mid-length and narrows both proximally and distally, a feature that *Yinlong* shares with *Stenopelix*.

Pubis. The pubis is well preserved in IVPP V14530 and IVPP V18684. It consists of the main body, the robust prepubic process and the short postpubic shaft (Figs 2B, 11B, D). The main body expands transversely to form a tight, subtriangular articulation with the ilium. Caudally, the pubic body forms the thin, curved cranioventral margin of the acetabulum.

The prepubic process is transversely expanded and dorsoventrally compressed, as in other basal ceratopsians (You *et al.* 2003; Averianov *et al.* 2006). This is unlike basal ornithischians (e.g. *Lesothosaurus*) and ornithopods (e.g. *Hypsilophodon*) which have dorsoventrally tall but mediolaterally compressed prepubes (Galton 1974; Baron *et al.* 2017). The dorsal surface of the prepubic process is slightly convex. In dorsal view the medial margin is straight; the lateral margin curves medially towards its distal end. The prepubic process is similar to that of *Auroraceratops* and *Archaeoceratops*, although the prepubes in the latter taxa are more slender (Fig. 11B, D). A deep, elongate notch is present on the dorsolateral margin of the base of the prepubic process (Figs 2B, 11B, D) and seems to be unique in *Yinlong downsi*.

The prepubic process is shorter than the preacetabular process of the ilium, as in other ceratopsians, such as *Auroraceratops* (Morschhauser 2012). The postpubic shaft extends caudally in line with the prepubic process (Xu *et al.* 2006). It is slender, subround in cross section, less than half the length of the ischial shaft, and tapers distally with an oval cross section, as in other ceratopsians, such as *Auroraceratops* (Morschhauser 2012). In other basal ornithischians, including *Lesothosaurus* (Baron *et al.* 2017), *Heterodontosaurus* (Santa Luca 1980), *Hexinlusaurus* (He & Cai 1984) and *Agilisaurus* (Peng 1992), the postpubic shafts are equal to or longer than the ischia. There is no trace of an obturator foramen.

Hind limb.

Femur. Femora are well preserved in IVPP V14530, IVPP V18637 and IVPP V18678, although some aspects are still concealed in the matrix (Fig. 12). Reconstruction of the femur is based on the exposed portions of these elements. The femur is long, robust and bowed cranially. The greater and lesser trochanters are closely spaced but are not fused in most specimens. In the large specimen IVPP V18637, the greater and lesser trochanters are separated from each other by a deep cleft (Fig. 12G), although

this may due to distortion during preservation. The separation of the greater and lesser trochanters is also seen in *Auroraceratops* (Morschhauser 2012) and in basal ornithischians such as *Hexinlusaurus* (He & Cai 1984), *Agilisaurus* (Peng 1992) and *Eocursor* (Butler *et al.* 2007), whereas in *Psittacosaurus* the trochanters are separated by grooves (Averianov *et al.* 2006). The lesser trochanter is small and tapers dorsally. The greater trochanter is twice the width of the lesser trochanter with a slightly expanded dorsal end. The lateral surface of the trochanters is convex craniocaudally and the dorsal margin is smooth and slightly convex.

A short but robust vertical ridge is centred on the greater trochanter, just distal to the base of the lesser trochanter (IVPP V18677), as also occurs in some small ornithopods such as *Jeholosaurus* (Han *et al.* 2012). There is a moderately well-defined femoral neck that separates the femoral head from the trochanters; it has a slightly concave dorsal margin (Fig. 12E, F). This is common in basal cerapods, but is absent in *Heterodontosaurus* and *Hexinlusaurus* (He & Cai 1984; Norman *et al.* 2011). The femoral head is robust and slightly mediolaterally compressed, with a convex articular surface. No obvious ligament sulcus is present on the caudal surface of the femoral head.

The shaft of the femur is robust and has a subtriangular cross section, narrowing to the cranial surface. A prominent pendant fourth trochanter is present on the caudomedial edge of the proximal part of the shaft. It is thin dorsally and thickened ventromedially. The dorsal edge is convex and narrow whereas the ventral margin is flattened. The entire fourth trochanter is straight and pendant in IVPP V18637, as in other ornithischians, but curved and strongly pendant in IVPP V14530 and IVPP V18679 (Fig. 12), which is similar to the basal ornithopods *Koreanosaurus* (Huh *et al.* 2011) and *Haya* (Makovicky *et al.* 2011). A shallow fossa is present at the cranial base of the fourth trochanter in IVPP V18678. Distally, the femur expands in all directions into robust inner and outer condyles which are divided by a deep popliteal fossa on the caudal surface (Fig. 12H). The extensor fossa on the cranial surface is shallow. The inner condyle is transversely expanded with a convex articular surface. The outer condyle is compressed transversely. A small fibular condyle extends caudally from the outer condyle, and extends slightly beyond the inner condyle (IVPP V18678). The articular surfaces of the distal condyles face caudoventrally when the femoral shaft is held vertically.

Tibia. The long, stout tibia is well preserved in IVPP V14530, IVPP V18637 and IVPP V18677 (Fig. 13). The ratio of the tibia to the femur is 1.1 in IVPP V18677 and 1.06 in IVPP V18684. This is similar in proportion to *Psittacosaurus*, and the neoceratopsians *Protoceratops*, *Leptoceratops* and *Montanoceratops*, but is lower than the
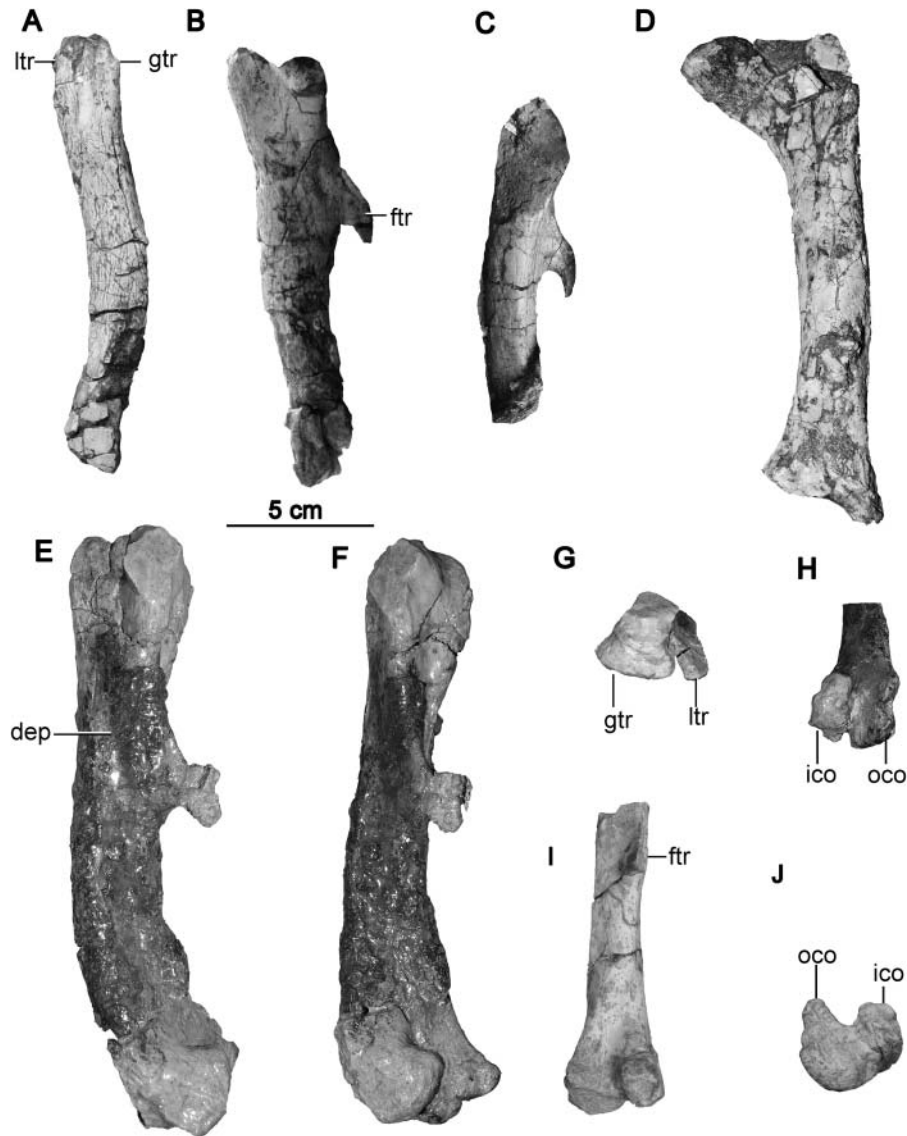
Figure 12. Photographs of femora of *Yinlong downsi*. **A, B,** IVPP V14530, right femur in **A,** lateral view; **B,** cranial view. **C,** IVPP V18679, right femur in medial view. **D,** IVPP V18684, left femur in cranial view. **E–H,** IVPP V18637; right femur in **E** medial view; **F,** caudomedial view; **G,** dorsal view; **H,** caudoventral view. **I, J,** IVPP V18678; left femur in **I,** caudal view; **J,** distal view. Abbreviations: dep, depression; ftr, fourth trochanter; gtr, greater trochanter; ico, inner condyle; ltr, lesser trochanter; oco, outer condyle.

ratio in *Heterodontosaurus* (1.3, Sereno 1987), *Lesothosaurus* (1.25, Baron *et al.* 2017), and the ornithopod *Jeholosaurus* (1.16–1.40, Han *et al.* 2012). In *Stenopelix* and Pachycephalosaurs, the tibia is relatively equal to or shorter than the femur (Sereno 1987). The proximal end of the tibia is expanded craniocaudally and consists of the tibial platform, the inner condyle, the cranial fibular condyle and the cnemial crest. The tibial platform narrows caudally to form the inner condyle, which projects caudally beyond the shaft. The inner condyle is oriented caudolaterally. The well-developed fibular condyle is centred on the proximal end, and expands laterally into a rounded process (Fig. 13C), but it projects more caudally in the large individual IVPP V18637 (Fig. 13F). The tibial platform narrows slightly cranially to form a blunt cnemial crest. On the caudal surface, a shallow sulcus runs between the fibular condyle and the inner condyle. The shaft of the tibia is transversely narrowest at mid-length and has an oval cross section. Distally, the tibia expands mediolaterally to form the medial and lateral malleoli (Fig. 13E, G). The lateral malleolus is nearly twice the width of the medial malleolus. On the cranial surface they are separated by a broad and shallow sulcus. A moderately strong ascending ridge separates them on the caudal surface, giving the tibia an asymmetrical triangular shape in distal view (Fig. 13G). The lateral malleolus extends further
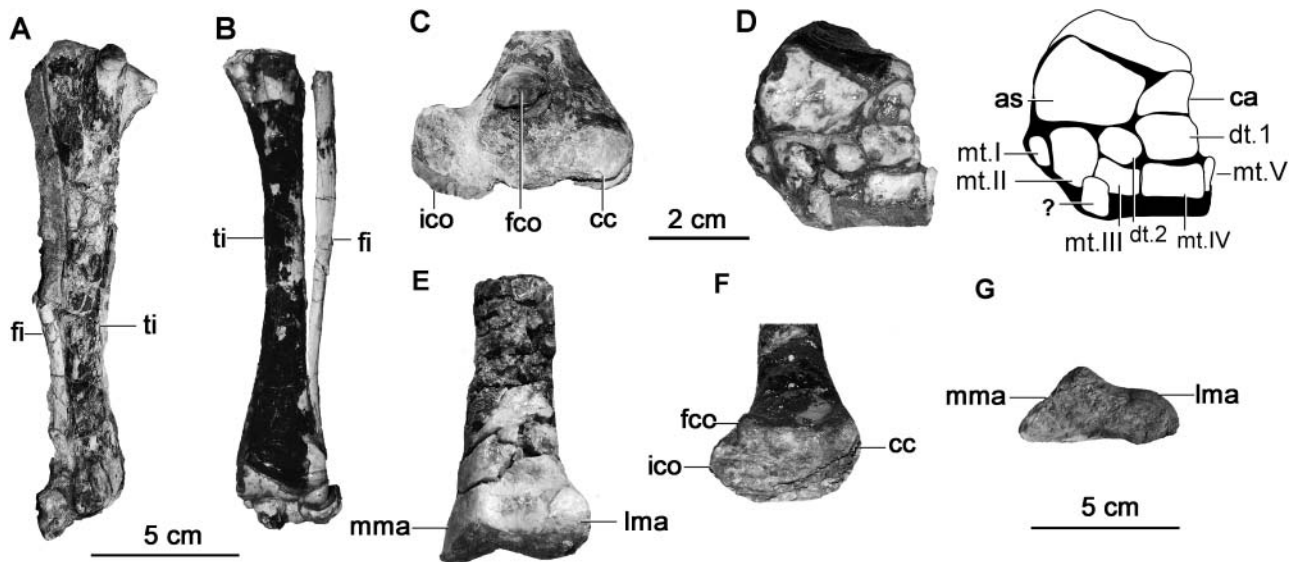
Figure 13. Photographs of tibiae and fibulae of *Yinlong downsi*. **A–D,** IVPP V18677; **A,** left tibia and fibula in cranial view; **B,** right tibia and fibula in caudal view; **C,** left tibia in proximal view; **D,** distal view showing the calcaneum, astragalus, distal tarsals and proximal metatarsals. **E–G,** IVPP V18637; **E,** distal half of the tibia in caudal view; **F,** tibia in proximal view; **G,** tibia in distal view. Abbreviations: as, astragalus; ca, calcaneum; cc, cnemial crest; dt, distal tarsal; fco, fibula condyle; fi, fibula; ico, inner condyle; lma, lateral malleolus; mma, medial malleolus; mt, metatarsal; ti, tibia.

distally than the medial. The cranial surface of the medial malleolus is smooth and flat. The craniolateral surface of the lateral malleolus is flattened to articulate with the distal fibula.

Fibula. The fibula is articulated with the tibia in IVPP V14530 (Fig. 13B, D). The fibula is long and narrow, and approximately 25% the width of the tibia at their narrowest points, whereas in heterodontosaurids *Fruitadens* and *Heterodontosaurus* the distal half of the fibula is more strongly reduced (Butler *et al*. 2012). The proximal end is expanded craniocaudally and compressed mediolaterally. The fibular shaft becomes progressively narrower distally and is narrowest near the distal end. It curves medially, towards the tibia, beginning at mid-shaft so that its distal end articulates with the craniolateral surface of the lateral malleolus. The distal fibula expands slightly cranially.

Proximal tarsals. The astragalus and calcaneum are articulated and moderately well preserved in IVPP V18677 (Fig. 13B, D). However, the cranial surface is concealed by the flexure of the pes on the crus. The astragalus is twice the width of the calcaneum and both elements are tightly fit to the crus. The astragalus and the calcaneum contact each other along a tight, craniomedially directed suture but are not fused with each other, unlike in heterodontosaurids (Butler *et al.* 2010). In caudal view, the astragalus is wedge-shaped in outline as it extends proximally between the malleoli up to the ascending ridge of the tibia. The astragalus has a slightly concave

medial surface, and the distal surface is roller-like. The calcaneum is subtriangular in distal view, narrowing medially. Its lateral surface is significantly concave, whereas the distal and caudal surfaces are rounded. Generally, their shapes are similar to basal ornithopods, such as *Jeholosaurus* (Han *et al*. 2012).

Distal tarsal. Two laterally placed, unfused distal tarsals are preserved in articulation on IVPP V18677 and can only be seen in caudal view (Fig. 13D). In caudal view, the lateralmost distal tarsal is sub-rectangular in outline and nearly twice the size of the oval medialmost distal tarsal. The lateralmost distal tarsal is located between the calcaneum and the fourth metatarsal. The medialmost distal tarsal intercedes between the lateral astragalus and the third metatarsal. The medial surface of the lateralmost distal tarsal is slightly concave to receive the more rounded lateral surface of the adjacent distal tarsal. The tight articulation between the two distal tarsals extends craniocaudally and intersects the suture between the astragalus and calcaneum.

Most ornithischians have two distal tarsals, including *Lesothosaurus* (Sereno 1991), *Hexinlusaurus* (He & Cai 1984), *Scelidosaurus* (Norman 2001), the basal ceratopsian *Auroraceratops* (Morschhauser 2012) and the basal ornithopods *Hypsilophodon* (Galton 1974) and *Jeholosaurus* (Han *et al.* 2012). However, the medialmost distal tarsal is much smaller than the lateralmost distal tarsal in *Yinlong*, and articulates only with metatarsal III, unlike basal ornithopods such as *Jeholosaurus* (Han *et al.* 2012) and the basal neoceratopsian *Auroraceratops* (Morschhauser 2012),
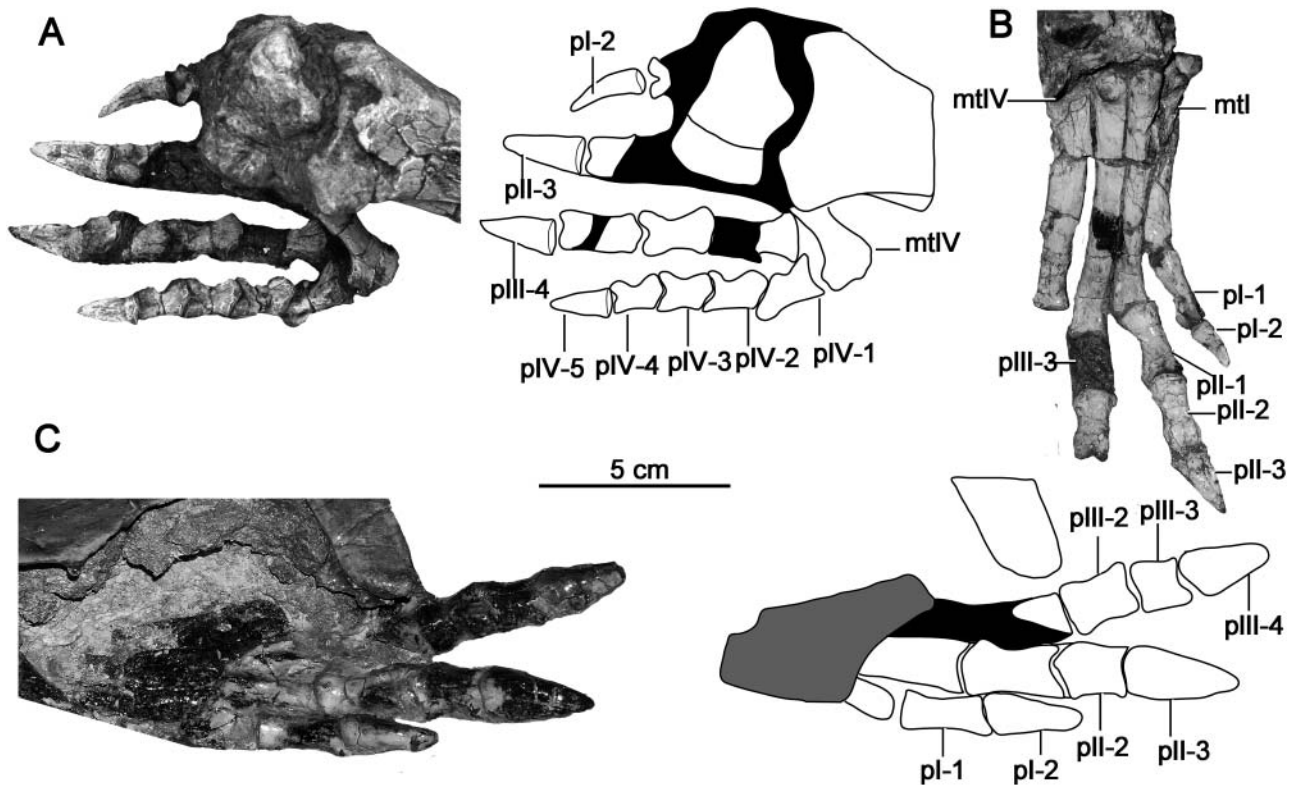
Figure 14. Photographs and line drawings of pedes of *Yinlong downsi*. **A,** IVPP V14530, pes in ventral view. **B,** IVPP V18677, left pes in ventral view. **C,** IVPP V18637, left pes in dorsal view. Abbreviations: pI-IV, pedal digit I- IV; mt, metatarsal.

where it articulates with metatarsals III and IV. Three distal tarsals are present in *Heterodontosaurus*, some iguanodontians (e.g. *Iguanodon*) and some ceratopsids, such as '*Brachyceratops*' (Gilmore 1917), but are unknown in ankylosaurs and stegosaurs (Galton & Upchurch 2004; Vickaryous *et al.* 2004).

Pes. The pes is well preserved in IVPP V14530, IVPP V18677, IVPP V18685 and IVPP V18637 (Fig. 14). The metatarsals are long and slender, contacting each other along their shafts for nearly their entire lengths. All the metatarsals (MT) lie in the same plane and are expanded at both their proximal and distal ends. The dorsal surfaces are convex and the plantar surfaces are flattened. Metatarsal III is the longest. MT II is 10% shorter than MT III (IVPP V18677), and MT IV is 30% shorter than MT III (IVPP V18677 and IVPP V14530). Metatarsal I is 65% the length of MT III, which is similar to the basal ceratopsians *Psittacosaurus* (69%, Averianov *et al.* 2006) and *Auroraceratops* (63%, Morschhauser 2012). MT I is more reduced and only half the length of MT III in *Heterodontosaurus* (55%, Sereno 2012), *Agilisaurus* (53%, Peng 1992), and many ornithopods such as *Jeholosaurus* (Han *et al.* 2012). However, in *Lesothosaurus*, Metatarsal I is less than half the length of Metatarsal II in the small specimen NHMUK PVRUB17, but their ratio reaches 70% in

the large specimen (SAM-PK-K1105) (Baron *et al.* 2017), suggests that this ratio may change significantly during ontogeny.

The shaft of MT I is straight and articulates proximally with the astragalus. It is dorsoventrally expanded at its proximal end. The shafts of MT I and II are equal in width, as occurs in *Psittacosaurus* (Averianov *et al.* 2006), whereas in the basal neoceratopsians *Archaeoceratops* (IVPP V11114) and *Auroraceratops*, the shaft of MT1 is narrow transversely along the proximal half (You & Dodson 2003; Morschhauser 2012). Metatarsal I is tightly held against MT II for its entire length; the surface of the medial condyle is thickened and flattened to lie against MT II.

Metatarsal II is straight and maintains the same width along its entire length. The proximal end is dorsoplantarly expanded and mediolaterally compressed. The distal end of MT II is slightly transversely expanded and its condyles are separated by a shallow intercondylar sulcus. The surface of the lateral condyle is closely appressed to the shaft of MT III.

The shaft of MT III is very slightly bowed medially. The proximal end is strongly expanded dorsoplantarly, and compressed mediolaterally. The medial surface of the shaft is tightly appressed to MT II along their entire lengths. Laterally, MT IV contacts only the proximal half

of the shaft of MT III. Distally, MT III expands slightly into two condyles that are weakly divided by an intercondylar sulcus.

The shaft of MT IV curves slightly laterally for most of its length; the distal one-third of the metatarsal curves slightly medially back towards MT III but does not meet it. The medial surface of the curving shaft meets MT III for only its proximal half. The proximal end is strongly expanded transversely, compressed dorsoplantarly, and narrowed laterally. The shaft is the widest among all of the metatarsals, but narrows distally. The distal end is expanded slightly to a single condyle.

Metatarsal V is only preserved in IVPP V18677 (Fig. 13D). It is mediolaterally compressed and tightly appressed to MT IV. The distal part is concealed in the matrix and not visible.

The pedal phalanges are well preserved and articulated in IVPP V14530, IVPP V18637 and IVPP V18677. The phalangeal formula is 2-3-4-5-0. In the following description, the phalanges are described in plantigrade stance.

All of the non-ungual phalanges are similar to each other except phalanx I-1. The latter is more slender than other phalanges, the proximal articular surface is concave and lacks division, and the distal end extends beyond that of MT II (Fig. 14B), as in other ceratopsians (e.g. *Psittacosaurus*, Averianov *et al.* 2006). The phalanges are slender in small individuals (Fig. 14B), but more robust in larger ones (Fig. 14C). The dorsoventral depth of the phalanges is less than their transverse width, and they both are exceeded by their length. This differs from basal ornithopods whose phalanges have relatively equal width and depth (e.g. *Jeholosaurus*, Han *et al.* 2012). The non-ungual phalanges are expanded both proximally and distally. The proximodorsal ends of the phalanges extend caudally between the preceding condyles, covering the concave articular surface of the preceding phalanges. This is more prominent in distal phalanges.

The proximal articular surfaces of the phalanges are separated into medial and lateral portions by a vertical ridge for articulation with the ginglymi of the preceding elements. The distal phalanges are divided into lateral and medial condyles, with deep ligament pits laterally. The expansion of the proximal ends is greater than on the distal ends.

The unguals are dorsoplantarly flattened, and the plantar surfaces are concave (Fig. 14). A weak ridge extends longitudinally along the ventral surface of each ungual. The distal end tapers and curves slightly plantarly. The second ungual is the most robust. The first and third unguals are relatively equal in length, but the former is narrower than the latter. The fourth ungual is the smallest. Sulci are present on the lateral surfaces of all the unguals. In overall morphology, the pes of *Yinlong* is similar to other ceratopsians, such as *Psittacosaurus* and *Auroraceratops* (Averianov *et al.* 2006; Morschhauser 2012),

and unlike that of ornithopods, which is slenderer and has more dorsoplantarly expanded elements (Han *et al.* 2012).

Discussion

Phylogenetic analysis

The addition of postcranial characters to phylogenetic analyses, which are often biased towards dental and cranial characters, has been shown to improve resolution in phylogenetic analyses (Mounce *et al.* 2016). However, there has been no detailed information from the postcranial skeleton of chaoyangsaurid basal ceratopsians. With this description of the postcranial skeleton of *Yinlong*, we reassess the systematic position of *Yinlong downsi* within Marginocephalia, the arrangement of taxa at the base of Ceratopsia, and the arrangement of taxa at and near the base of Ornithischia, by compiling and analysing a new character list and matrix. Our data matrix is based on those of Maryańska & Osmólska (1985), Sereno (1986, 1999), Weishampel & Heinrich (1992), Weishampel *et al.* (2003), Cooper (1985), Forster (1990), Norman (2002), Xu *et al.* (2002, 2006), Hill *et al.* (2003), Butler *et al.* (2008, 2011), Boyd (2015) and Han *et al.* (2015). Eighteen new characters were added based on direct observation (Supplemental Appendix 3, marked with *). The codings for *Huayangosaurus*, *Haya*, *Jeholosaurus*, *Psittacosaurus*, *Tianyulong*, *Yinlong*, *Archaeoceratops*, *Liaoceratops*, *Xuanhuaceratops* and *Chaoyangsaurus* were based on first-hand observation (Supplemental Appendix 4). The character list is provided in Supplemental Appendix 3. Three hundred and twenty-five comparative figures are provided in order to make the character states more easily visualized. The new data matrix is available as supporting information (note that an all zero dummy character was added at the beginning of the matrix to aid with interpretation because TNT numbers characters beginning with '0'). It was constructed using Mesquite v.2.75 (Maddison & Maddison 2011).

The final data matrix consists of 380 characters scored for 68 ingroup taxa. There are 226 cranial characters and 154 postcranial characters. Four outgroups were chosen to accurately polarize characters. The outgroup taxa include the non-dinosaurian dinosauromorph *Marasuchus lilloensis* (Romer 1972; Sereno & Arcucci 1994), the basal ornithodiran *Silesaurus opolensis* (Dzik 2003; Nesbitt 2011), the basal sauropodomorph *Eoraptor lunensis* (Martinez *et al.* 2011; Sereno *et al.* 2013), and the basal saurischian *Herrerasaurus ischigualastensis* (Reig 1963; Novas 1993; Sereno 1994; Langer *et al.* 2010).

The matrix was analysed using TNT (Goloboff *et al.* 2008), and all characters were treated as equally weighted. Twenty-one characters (2, 23, 31, 39, 125, 163, 196, 203, 204, 222, 227, 238, 243, 247, 268, 292, 296, 302, 306, 320, 361) were treated as ordered (additive) because they

form transformation series. The analysis was conducted with the maximum trees set to 99,999 and zero-length branches collapsed, using a heuristic search with 1000 replicates of tree bisection and reconnection holding 100 trees with each replicate, followed by tree swapping using TBR on the trees in RAM. Standard bootstrap values (absolute frequencies) were calculated using a traditional heuristic search (1000 replicates of TBR each bootstrap replicate, 10 trees saved per TBR) with 100 bootstrap replications. Bremer supports were calculated by running the script 'Bremer.run'. Unstable taxa were identified by using the command 'pruned trees' up to eight unstable taxa, including *Pisanosaurus*, *Laquintasaurua*, *Micropachycephalosaurus*, *Zephylosaurus*, *Yueosaurus*, *Albalophosaurus* and *Koreaceratops*. The reduced consensus tree shows relationships among the remaining taxa after these eight taxa are removed from the most parsimonious tree topologies, and the bootstrap and Bremer support values were obtained after excluding these eight taxa in new bootstrap and Bremer support analyses.

The analysis produced 53,376 most parsimonious trees of 1211 steps, a consistency index (CI) of 0.37 and retention index (RI) of 0.71. Though the strict consensus tree shows poor resolution in some areas (Fig. 15), it supports most clades established in previous analyses, including Ornithischia, Neoceratopsia, Ceratopsia, Chaoyangsauridae, Iguanodontia, Ankylosauria, Stegosauria, Pachycephalosauria, Heterodontosauridae and Thyreophora. However, it does not support the monophyly of Genasauria, Cerapoda and Marginocephalia, and many taxa previously considered basal ornithopods, such as *Jeholosaurus*, *Hypsilophodon* and *Haya*, were moved to the base of Neornithischia. Using the reduced consensus method provides a more resolved picture of ornithischian relationships, especially small basal ornithopods (Fig. 16). The reduced consensus tree also supports the monophyly of chaoyangsaurids and *Psittacosaurus* (Han *et al.* 2016). The bootstrap and Bremer support values are high in groups nested within the tree, including Thyreophora, Ankylosauria, Stegosauria, Iguanodontia, *Psittacosaurus* and Neoceratopsia, but are weak in basal ornithischians, basal ornithopods, chaoyangsaurids and heterodontosaurids.

In the strict consensus, *Lesothosaurus*, *Eocursor*, *Pisanosaurus* and *Laquintasaura* form a polytomy with heterodontosaurids and Thyreophora at the base of Ornithischia, whereas the reduced consensus analysis supports only *Eocursor* and heterodontosaurids to be the most basal ornithischians among stable relationship. This is in contrast to the analysis of Boyd (2015), which placed *Eocursor* with heterodontosaurids. *Lesothosaurus* was placed at the base of genasaurians for the first time, but there are no unambiguous synapomorphies to support this clade. The monophyly of heterodontosaurids is well supported and the group is at the base of Ornithischia in both the strict and reduced consensus trees. Two

synapomorphies support their monophyly: coronoid process is well developed, depth of mandible at coronoid is more than 150% depth of mandible beneath tooth row (174:1), which is convergent with neornithischians; and distal end of the fibula is strongly reduced and splint like (363:1). This feature was recognized by Butler *et al.* (2010, 2012) and seems to be convergent with pachycephalosaurs (Sereno 2000). The new analysis put *Abrictosaurus* as the most basal heterodontosaurid, as in Norman *et al.* (2011), unlike in Sereno (2012). Additionally, *Echinodon* was found to be a basal heterodontosaurid by Sereno (2012), but here it is recovered with *Heterodontsaurus* and *Pegomastax*. The relationships within Heterodontosauridae are weakly supported and need more work.

The new analysis includes many basal ceratopsians that were absent in previous ornithischian phylogenetic analyses, and greatly improves our understanding of the relationships of basal ceratopsians. The Chaoyangsauridae including *Yinlong*, *Chaoyangsaurus*, *Stenopelix*, *Xuanhuaceratops* and *Hualianceratops* is present in the strict consensus, although only *Xuanhuaceratops* and *Hualianceratops* form a group if the characters are all unordered. Three unambiguous synapomorphies support chaoyangsaurid monophyly in the strict consensus, including the absence of a prominent primary ridge on the labial side of maxillary teeth (209:0) and any apicobasally extending ridges on cheek teeth (207:0; 210:0). However, the bootstrap and Bremer support is very low, possibly affected by the unstable taxon *Albalophosaurus*. In the reduced consensus, the Bremer support value is 2, and seven synapomorphies support this clade: sculpted ornamentation on lateral surface of the jugal-postorbital-angular (57:1), a distinct groove present on the ventral margin of the quadratojugal for articulating with the caudal ramus of the jugal (66:1), an enlarged tubercle row on caudal edge of the squamosal (117:1), the dorsal surface of the squamosal strongly expanded in dorsal view (118:1), medial expansion of the glenoid in articular forming a semilunar surface (190:1), absence of apicobasally extending ridges on check teeth (207:0), and scapula elongate, length at least nine times the minimum width (268:0). Most of these features are discussed by Han *et al.* (2015, 2016) and seem to be unique among Ornithischians.

The taxa within Thyreophora are quite stable as in previous phylogenetic analyses. Here, a new basal neornithischian, *Isaberrysaura mollensis* from the Jurassic of South America, was included in the new phylogenetic analysis (Salgado *et al.* 2017). *Isaberrysaura* was found to be a basal ornithopod previously (Salgado *et al.* 2017) although it preserved some stegosaur features. Here it was recovered as a basal stegosaur for the first time. Thirteen synapomorphies (80:1, 91:1, 100:0, 147:0, 191:1, 240:1, 250:1, 252:1, 260:1, 281:1, 307:1, 341:1, 346:1) support its assignment to Stegosauria. Two synapomorphies support *Isaberrysaura* and *Huayangosaurus* as sister taxa:
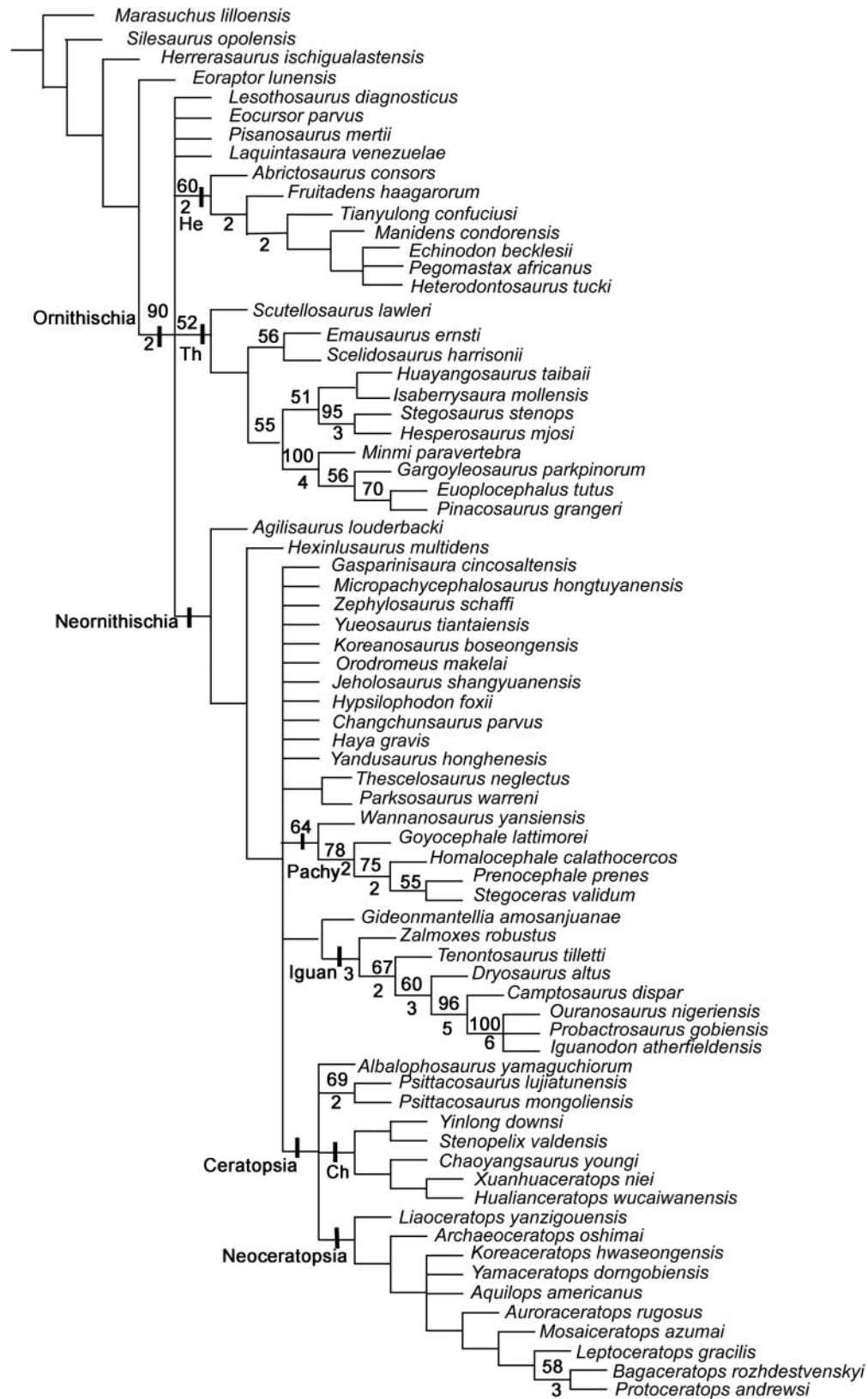
Figure 15. Strict consensus of 53,376 most parsimonious trees (MPTs) produced by analysing a data matrix of 72 taxa and 380 characters. Values above nodes represent bootstrap proportions. Values beneath nodes indicate Bremer support. Bremer support values of 1 are not shown. Abbreviations: Ch, Chaoyangsauridae; He, Heterodontosauridae; Iguan, Iguanodontia; Pachy, Pachycephalosauria; Th, Thyreophora.
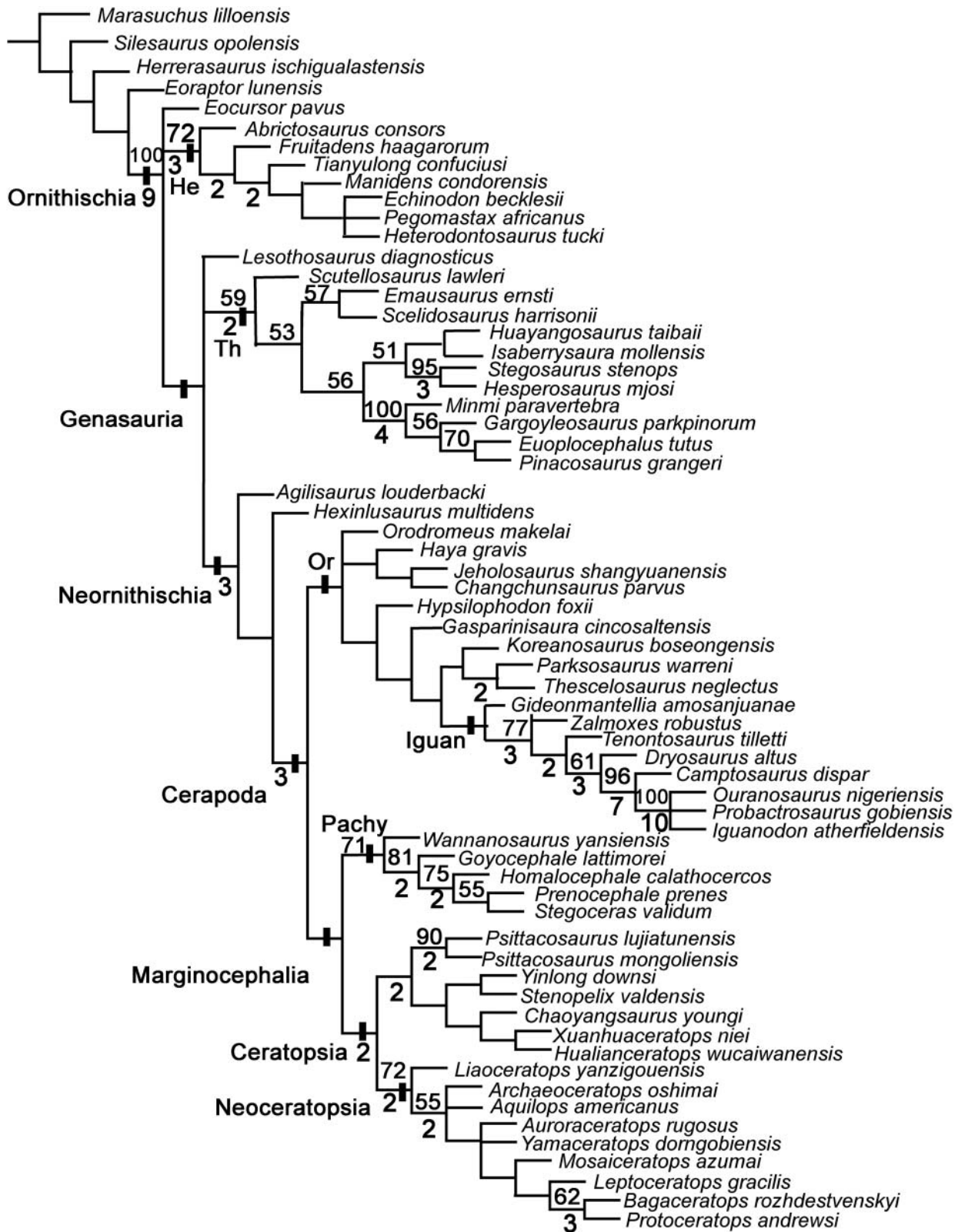
Figure 16. Reduced consensus tree derived by *a posteriori* pruning of eight unstable taxa (*Yueosaurus*, *Pisanosaurus*, *Yandusaurus*, *Zephylosaurus*, *Albalophosaurus Laquintasaura*, *Micropachycephalosaurus* and *Koreaceratops*) from 53,376 most parsimonious trees generated by the full analysis. Values above nodes represent bootstrap proportions. Values beneath nodes indicate Bremer support. Bremer support values of 1 are not shown. Abbreviations: Ch, Chaoyangsauridae; He, Heterodontosauridae; Iguan, Iguanodontia; Or, Ornithopoda; Pachy, Pachycephalosauria; Th, Thyreophora.

fossa-like depression positioned on the premaxillary (15:1) and deep elliptical fossa present along sutural line of the nasals (26:1).

The taxa usually considered basal ornithopods are completely unresolved in the strict consensus tree. However, in the reduced consensus tree their relationships are much more resolved though weakly supported based on bootstrap and Bremer support values. This analysis supports the validity of Jeholosauridae (*Jeholosaurus*, *Changchunsaurus* and *Haya*; see Han *et al*. 2012) and the monophyly of *Koreanosaurus*, *Parksosaurus* and *Thescelosaurus*, both placed at the base of Ornithopoda outside of Iguanodontia. This contrasts with the phylogeny of Boyd (2015) that put these taxa outside Cerapoda and recovered *Hypsilophodon* to be the only non-iguanodont ornithopod. Here, four synapomorphies support the monophyly of ornithopods: the presence of a fossa-like depression on the premaxilla-maxilla boundary (15:1), pterygoid mandibular process short, terminates at or above maxillary tooth row (140:1), predentary long and about equal in length to the premaxilla (154:1), and prominent femoral ligament sulcus (351:1). The monophyly of Jeholosauridae is weakly supported, by two characters: jugal caudal ramus forked (63:1) and a long ischium symphysis (335:0). Boyd (2015) listed several features that distinguish *Jeholosaurus* from *Haya* and *Changchunsaurus* based on *Jeholosaurus* specimens housed at Peking University. However, at least two of these features are actually variable for *Jeholosaurus*. Boyd (2015) described the rostral tip of the dentary as being near its ventral margin and the ventral and dorsal margins of the dentary converging rostrally in *Jeholosaurus*. This is not obvious on the *J. shangyuanensis* holotype IVPP V12529 and large specimens IVPP V15716 and IVPP V15717. Moreover, contrary to Boyd (2015), some dentary teeth preserve primary ridges as in *Haya* and *Changchunsaurus* (*Jeholosaurus* IVPP V12530). Therefore, these features do not differ in *Jeholosaurus*, *Haya* and *Changchunsaurus*, and it is possible that the Asian small ornithopods form a group.

Yinlong downsi provides more evidence to support the monophyly of Marginocephalia (Xu *et al.* 2006), but this is not supported by the strict consensus tree. However, Marginocephalia are monophyletic in the reduced consensus tree, which is supported by 15 unambiguous synapomorphies (84:1, 103:1, 110:1, 114:1, 129:1, 132:1, 135:1, 139:1, 193:2, 196:3, 244:1, 311:1, 320:2, 333:0, 338:1), although the bootstrap values and Bremer support are weak. All these features were recognized by previous studies. Our analysis does not support the monophyly of heterodontosaurids and marginocephalians found by Xu *et al.* (2006), in agreement with most previous analyses (Butler *et al.* 2008; Norman *et al.* 2011; Boyd 2015). They may share one potential synapomorphy (three premaxillary teeth), but it is too weak to support their monophyly (Norman *et al.* 2011). The postcranial material of

Yinlong downsi is also significantly different from that of heterodontosaurids, providing more evidence that they do not form a natural group or clade. Additionally, all definitive pachycephalosaurs come from the Late Cretaceous and are all highly specialized, making their relationship with ceratopsians still weakly supported. The discovery of early pachycephalosaurs should help to solve this problem.

Stenopelix was found to be the sister taxon of *Yinlong*, as suggested by Butler *et al*. (2011). This is supported by the deep notch separating the lesser and greater trochanters (354:0). The holotype of *Spenopelix valdensis* from the 'Wealden' Lower Cretaceous of north-western Germany includes only postcranial material, and its phylogenetic position has been ambiguous. It has been hypothesized to be a pachycephalosaur (Sues & Galton 1982; Maryańska *et al.* 2004; Butler & Sullivan 2009), but recently Butler *et al.* (2011) found it to be the sister taxon of *Yinlong* in their 50% majority rule consensus tree, although they did not discuss this relationship. Here we found that *Stenopelix* and *Yinlong* are very similar to each other in postcranial elements, especially the pelvic girdle. However, the femur is longer than the tibia in *Stenopelix*, unlike all basal ceratopsians (Butler & Sullivan 2009). Skull elements of *Stenopelix* would be very important to clarifying its position.

Psittacosaurus is a specialized group of ceratopsians found only in the Early Cretaceous of Asia (Sereno 2010). They bear many unique features, and they were not placed within Ceratopsia until the rostral bone was identified (Maryańska & Osmólska 1975). *Psittacosaurus* are quite different from all other ceratopsians, suggesting an early divergence between them (Sereno 2010). The basal ceratopsians from China, especially *Yinlong downsi*, provide more evidence that *Psittacosaurus* is a ceratopsian, but recent phylogenetic analyses put *Psittacosaurus* in three different positions within the group. Some studies indicated that *Psittacosaurus* is still the most basal ceratopsian, and chaoyangsaurids and Neoceratopsia are more closely related to each other (Sereno 2000; Morschhauser 2012). Other studies support *Yinlong* and *Chaoyangsaurus* as the most basal ceratopsian (Xu *et al.* 2006; Zheng *et al.* 2015). However, after a detailed study of *Yinlong* and other basal ceratopsians, Han *et al.* (2015, 2016) found many features that are shared by chaoyangsaurids and *Psittacosaurus*, such as the maxillary ramus of the jugal much shorter than the quadratojugal ramus, the transversely expanded ventral surface of the jugal, the relatively equal length of the surangular and angular and the new basal ceratopsian phylogenetic analysis, support their monophyly. Here, their close relationship is well supported by the reduced consensus tree though the bootstrap value and Bremer support are still low. Eleven synapomorphies support their relationship: preorbital skull length less than 35% of basal skull length (2:2), subtemporal

length more than 45% of basal skull length (3:1), rostral ramus of the jugal deeper (52:2) and shorter (53:3) than caudal ramus, the caudal ramus of the jugal strongly arched laterally (60: 1), forked at the distal end (63:1), extending to the ventral margin of the quadratojugal (65:5), infratemporal fenestra larger than the orbital (100:0), surangular length more than 50% of mandibular length (183:1), angular ventral margin straight and caudodorsally extending (193:1) and scapular blade dorsal margin relatively straight (273:0). However, synapomorphies are concentrated in the jugal, postorbital, quadrate and the mandible, whereas the rostral part of the skull and the basal tubera of *Yinlong* are more similar to neoceratopsians, such as *Liaoceratops* and *Archaeoceratops*.

The position of *Mosaiceratops* in this analysis is closer to coronosaurians than in a previous analysis (Zheng *et al.* 2015). *Mosaiceratops* from the Upper Cretaceous of central China was regarded as a basal neoceratopsian outside of Coronosauria by Zheng *et al.* (2015), and it was considered to preserve three features that were previously unique to *Psittacosaurus*. However, all these features are ambiguous. The external naris is not positioned as high as in *Psittacosaurus*; it is more similar to the position in the neoceratopsian *Protoceratops* (Brown & Schlaikjer 1940; Lambert *et al.* 2001). The ventrally extending nasal articulating with the rostral is unique to *Psittacosaurus*, but it is not clearly present in *Masaiceratops* due to damage to this area. Finally, the notch between the basal tubera is a primitive character of ornithischians that is also seen in *Heterodontosaurus* (Norman *et al.* 2011) and *Jeholosaurus* (Barrett *et al.* 2009), though not as prominent as in *Psittacosaurus* and *Mosaiceratops*. *Mosaiceratops* preserves two synapomorphies with leptoceratopsids and protoceratopsids: tip of predentary strongly upturned relative to main body of predentary (157:1) and absence of premaxillary teeth (195:1).

We explored the structure of the data matrix by constraining taxa to be in positions found in some earlier analyses. Constraining heterodontosaurids (*Abrictosaurus*, *Fruitadens*, *Tianyulong*, *Manidens*, *Echinodon*, *Pegomastax* and *Heterodontosaurus*) with marginocephalians results in trees only three steps longer. Furthermore, when chaoyangsaurids are constrained to be outside of other ceratopsians, also resulting in trees three steps longer, then heterodontosaurids are sister to Ceratopsia. In these trees *Stenopelix* is sister to Ceratopsia and other chaoyangsaurids are one node closer to other ceratopsians. When heterodontosaurids are constrained with marginocephalians they go with ceratopsians and are supported by the following synapomorphies: antorbital fossa ventral margin below that of the orbital (38:1), jugal participation in caudoventral margin of the antorbital fossa (50:0), jugal posterior process forked (63:1), presence of quadrate foramen (89:0), lateral quadrate condyle larger than the medial (92:2), frontal participation in supratemporal fenestra (93:1), presence of smooth depression on the caudal edge of the frontal (95:1), parietal sharp sagittal crest

(104:1), small fenestral positioned dorsally on the surangular–dentary joint (181:1), scapula blade elongate and strap-like (268:0) and prepubic process compressed medialaterally (344:0).

Cabreira *et al.* (2016) found silesaurids grouped with ornithischians, so we constrained *Silesaurus opolensis* to be more closely related to Ornithischia than are the other three outgroup taxa. The most parsimonious trees under this constraint are six steps longer (1217 steps) than in the unconstrained trees, and there are fewer most parsimonious trees (20,016). *Silesaurus* is in a basal trichotomy with *Pisanosaurus* in the strict consensus, because in fundamental trees either *Pisanosaurus* is closer to other ornithischians or it forms a clade with *Silesaurus* supported by one character, apicobasally extending ridges on lingual/labial surfaces of cheek teeth present (207:1). The Heterodontosauridae are sister to all other ornithischians, with *Eocursor* sister to the remaining ornithischians. *Lesothosaurus* and *Laquintasaura* are resolved as basal thyreophorans based on six or more premaxillary teeth (196:0), and *Lesothosaurus* is closer to thyreophorans based on a horizontal dorsal margin of the iliac blade (306:1). Relationships within other groups are not affected.

Acknowledgements

Supplemental material

Supplemental material for this article can be accessed at: https://doi.org/10.1080/14772019.2017.1369185

References

Averianov, A. O., Voronkevich, A. V., Leshchinskiy, S. V. & Fayngertz, A. V. 2006. A ceratopsian dinosaur *Psittacosaurus sibiricus* from the Early Cretaceous of West Siberia, Russia and its phylogenetic relationships. *Journal of Systematic Palaeontology*, **4**, 359–395.

Baron, M. G., Norman, D. B. & **Barrett, P. M.** 2017. Postcranial anatomy of *Lesothosaurus diagnosticus* (Dinosauria: Ornithischia) from the Lower Jurassic of southern Africa: implications for basal ornithischian taxonomy and systematics. *Zoological Journal of the Linnean Society*, **179**, 125–168.

Barrett, P. M., Butler, R. J., Wang, X.–L. & **Xu, X.** 2009. Cranial anatomy of the Iguanodontoid Ornithopod *Jinzhousaurus yangi* from the Lower Cretaceous Yixian Formation of China. *Acta Palaeontologica Polonica*, **54**, 35–48.

Barrett, P. M., Butler, R. J., Mundil, R., Scheyer, T. M., Irmis, R. B. & **Sánchezvillagra, M. R.** 2014. A palaeoequatorial ornithischian and new constraints on early dinosaur diversification. *Proceedings of the Royal Society of London, Series B*, **281**(1791), 20141147.

Boyd, C. A. 2015. The systematic relationships and biogeographic history of ornithischian dinosaurs. *PeerJ*, **3**, e1523.

Brown, B. 1914. *Leptoceratops*, a new genus of Ceratopsia from the Edmonton Cretaceous of Alberta. *Bulletin of the American Museum of Natural History*, **33**, 567–580.

Brown, B. & **Schlaikjer, E. M.** 1940. The structure and relationships of *Protoceratops. Annals of the New York Academy of Sciences*, **40**, 133–266.

Brown, B. & **Schlaikjer, E. M.** 1942. The skeleton of *Leptoceratops* with the description of a new species. *American Museum of Natural History Novitates*, **1169**, 1–16.

Butler, R. J. 2005. The 'fabrosaurid' ornithischian dinosaurs of the Upper Elliot Formation (Lower Jurassic) of South Africa and Lesotho. *Zoological Journal of the Linnean Society*, **145**, 175–218.

Butler, R. J. 2010. The anatomy of the basal ornithischian dinosaur *Eocursor parvus* from the lower Elliot Formation (Late Triassic) of South Africa. *Zoological Journal of the Linnean Society*, **160**(4), 648–684.

Butler, R. J. & **Sullivan, R. M.** 2009. The phylogenetic position of the Ornithischian dinosaur *Stenopelix valdensis* from the Lower Cretaceous of Germany and the Early Fossil Record of Pachycephalosauria. *Acta Palaeontologica Polonica*, **54**, 21–34.

Butler, R. J. & **Zhao, Q.** 2009. The small-bodied ornithischian dinosaurs *Micropachycephalosaurus hongtuyanensis* and *Wannanosaurus yansiensis* from the Late Cretaceous of China. *Cretaceous Research*, **30**, 63–77.

Butler, R. J., Smith, R. M. H. & **Norman, D. B.** 2007. A primitive ornithischian dinosaur from the Late Triassic of South Africa, and the early evolution and diversification of Ornithischian. *Proceedings of the Royal Society, Series B*, **274** (1621), 2041–2046.

Butler, R. J., Upchurch, P. & **Norman, D. B.** 2008. The phylogeny of the ornithischian dinosaurs. *Journal of Systematic Palaeontology*, **6**, 1–40.

Butler, R. J., Galton, P. M., Porro, L. B., Chiappe, L. M., Henderson, D. M. & **Erickson, G. M.** 2010. Lower limits of ornithischian dinosaur body size inferred from a new Upper Jurassic heterodontosaurid from North America. *Proceedings of the Royal Society, Series B*, **277**(1680), 375–381.

Butler, R. J., Jin, L.-Y., Chen, J. & **Godefroit, P.** 2011. The postcranial osteology and phylogenetic position of the small ornithischian dinosaur *Changchunsaurus parvus* from the Quantou Formation (Cretaceous: Aptian–Cenomanian) of Jilin Province, north-eastern China. *Palaeontology*, **54**, 667–683.

Butler, R. J., Porro, L. B., Galton, P. M. & **Chiappe, L. M.** 2012. Anatomy and cranial functional morphology of the small-bodied dinosaur *Fruitadens haagarorum* from the Upper Jurassic of the USA. *PLoS ONE*, **7**(4), e31556.

Chinnery, B. J. & **Weishampel, D. B.** 1998. *Montanoceratops cerorhynchus* (Dinosauria: Ceratopsia) and relationships among basal neoceratopsians. *Journal of Vertebrate Paleontology*, **18**, 569–585.

Cooper, M. R. 1985. A revision of the ornithischian dinosaur *Kangnasaurus coetzeei* Haughton, with a classification of the Ornithischia. *Annals of the South African Museum*, **95**, 281–317.

Dzik, J. 2003. A beaked herbivorous archosaur with dinosaur affinities from the early Late Triassic of Poland. *Journal of Vertebrate Paleontology*, **23**, 556–574.

Forster, C. A. 1990. The postcranial skeleton of the ornithopod dinosaur *Tenontosaurus tilletti. Journal of Vertebrate Paleontology*, **10**, 273–294.

Galton, P. M. 1974. The ornithischian dinosaur *Hypsilophodon* from the Wealden of the Isle of Wight. *Bulletin of the British Museum (Natural History), Geology Series*, **25**, 1–152.

Galton, P. M. & **Upchurch, P.** 2004. Stegosauria. Pp. 343–362 in D. B. Weishampel, P. Dodson & H. Osmólska (eds) *The Dinosauria*. 2nd edition. University of California Press, Berkeley.

Gilmore, C. W. 1917. *Brachyceratops*: a ceratopsian dinosaur from the Two Medicine Formation of Montana, with notes on associated fossil reptiles. *US Geological Survey, Professional Paper*, **103**, 1–45.

Goloboff, P. A., Farris, J. S. & **Nixon, K. C.** 2008. TNT, a free program for phylogenetic analysis. *Cladistics*, **24**, 774–786.

Han, F.-L., Barrett, P. M., Butler, R. J. & **Xu, X.** 2012. Postcranial anatomy of *Jeholosaurus shangyuanensis* (Dinosauria, Ornithischia) from the Lower Cretaceous Yixian Formation of China. *Journal of Vertebrate Paleontology*, **32**, 1370–1395.

Han, F.-L., Forster, C., Clark, J. & **Xu, X.** 2015. A new taxon of basal ceratopsian from China and the early evolution of Ceratopsia. *PLoS ONE*, **10**(12), e0143369.

Han, F.-L., Forster, C. A., Clark, J. M. & **Xu, X.** 2016. Cranial anatomy of *Yinlong downsi* (Ornithischia: Ceratopsia) from the Upper Jurassic Shishugou Formation of Xinjiang, China. *Journal of Vertebrate Paleontology*, **36**, e1029579.

He, X. & **Cai, K.** 1984. *The Middle Jurassic dinosaurian fauna from Dashanpu, Zigong, Sichuan. Volume 1. The ornithopod dinosaurs*. Sichuan Scientific and Technological Publishing House, Chengdu, 71 pp. [In Chinese with English summary.]

He, Y., Makovicky, P. J., Wang, K., Chen, S., Sullivan, C., Han, F.-L. & **Xu, X.** 2015. A new Leptoceratopsid (Ornithischia, Ceratopsia) with a unique ischium from the Upper Cretaceous of Shandong Province, China. *PLoS ONE*, **10** (12), e0144148.

Hill, R. V., Witmer, L. M. & **Norell, M. A.** 2003. A new specimen of *Pinacosaurus grangeri* (Dinosauria: Ornithischia) from the Late Cretaceous of Mongolia: ontogeny and phylogeny of ankylosaurs. *American Museum of Natural History Novitates*, **3395**, 1–29.

Huh, M., Lee, D.-G., Kim, J.-K., Lim, J.-D. & **Godefroit, P.** 2011. A new basal ornithopod dinosaur from the Upper Cretaceous of South Korea. *Neues Jahrbuch für Geologie und Paläontologie, Abhandlungen*, **259**, 1–24.

Lambert, O., Godefroit, P., Li, H., Shang, C.-Y. & **Dong, Z.-M.** 2001. A new species of *Protoceratops* (Dinosauria, Neoceratopsia) from the Late Cretaceous of Inner Mongolia (PR China). *Bulletin de l'Institut royal des sciences naturelles de Belgique, Sciences de la Terre*, **Supplement 71**, 5–28.

Langer, M. C., Ezcurra, M. D., Bittencourt, J. S. & **Novas, F. E.** 2010. The origin and early evolution of dinosaurs. *Biological Reviews*, **85**, 55–110.

Lee, Y. N., Ryan, M. J., & Kobayashi, Y. 2011. The first ceratopsian dinosaur from South Korea. *Naturwissenschaften*, **98**(1), 39–49.

Maddison, W. & Maddison, D. 2011. *Mesquite: a modular system for evolutionary analysis. Version 2.75.* Available at: http://mesquiteproject.org

Makovicky, P. J., Kilbourne, B. M., Sadleir, R. W. & Norell, M. A. 2011. A new basal ornithopod (Dinosauria, Ornithischia) from the Late Cretaceous of Mongolia. *Journal of Vertebrate Paleontology*, **31**, 626–640.

Mallon, J. C. & Holmes, R. 2010. Description of a complete and fully articulated chasmosaurine postcranium previously assigned to *Anchiceratops* (Dinosauria: Ceratopsia). Pp. 189–202 in M. J. Ryan, B. J. Chinnery-Allgeier, D. A. Eberth & P. E. Ralrick (eds) *New perspectives on horned dinosaurs*. Indiana University Press, Bloomington.

Marsh, O. C. 1890. Additional characters of the Ceratopsidae with notice of new Cretaceous dinosaurs. *American Journal of Science, Series 3*, **39**, 418–426.

Martinez, R. N., Sereno, P. C., Alcober, O. A., Colombi, C. E., Renne, P. R., Montanez, I. P. & Currie, B. S. 2011. A basal dinosaur from the dawn of the dinosaur era in southwestern Pangaea. *Science*, **331**, 206–210.

Maryańska, T. & Osmólska, H. 1974. Pachycephalosauria, a new suborder of ornithischian dinosaurs. *Palaeontologia Polonica*, **30**, 45–102.

Maryańska, T. & Osmólska, H. 1975. Protoceratopsidae (Dinosauria) of Asia. *Palaeontologia Polonica*, **33**, 133–181.

Maryańska, T. & Osmólska, H. 1985. On ornithischian phylogeny. *Acta Palaeontologica Polonica*, **30**, 137–150.

Maryańska, T., Chapman, R. E. & Weishampel, D. B. 2004. Pachycephalosauria. Pp. 464–477 in D. B. Weishampel, P. Dodson & H. Osmólska (eds) *The Dinosauria*. 2nd edition. University of California Press, Berkeley.

Morschhauser, E. M. 2012. *The anatomy and phylogeny of Auroraceratops (Ornithischia: Ceratopsia) from the Yujingzi Basin of Gansu Province, China*. Unpublished PhD thesis, University of Pennsylvania, 629 pp.

Mounce, R. C. P., Sansom, R. & Wills, M. A. 2016. Sampling diverse characters improves phylogenies: Craniodental and postcranial characters of vertebrates often imply different trees. *Evolution*, **70**, 666–686.

Nesbitt, S. J. 2011. The early evolution of archosaurs: relationships and the origin of major clades. *Bulletin of the American Museum of Natural History*, **352**, 1–292.

Norman, D. B. 2001. *Scelidosaurus*, the earliest complete dinosaur. Pp. 3–24 in K. Carpenter (ed.) *The armored dinosaurs*. Indiana University Press, Bloomington.

Norman, D. B. 2002. On Asian ornithopods (Dinosauria: Ornithischia). 4. *Probactrosaurus* Rozhdestvensky, 1966. *Zoological Journal of the Linnean Society*, **136**, 113–144.

Norman, D. B., Witmer, L. M. & Weishampel, D. B. 2004. Basal Thyreophora. Pp. 335–342 in D. B. Weishampel, P. Dodson & H. Osmólska (eds) *The Dinosauria*. 2nd edition. University of Californian Press, Berkeley.

Norman, D. B., Crompton, A. W., Butler, R. J., Porro, L. B. & Charig, A. J. 2011. The Lower Jurassic ornithischian dinosaur *Heterodontosaurus tucki* Crompton & Charig, 1962: cranial anatomy, functional morphology, taxonomy, and relationships. *Zoological Journal of the Linnean Society*, **163**, 182–276.

Novas, F. E. 1993. New information on the systematics and postcranial skeleton of *Herrerasaurus ischigualastensis* (Theropoda: Herrerasauridae) from the Ischigualasto Formation (Upper Triassic) of Argentina. *Journal of Vertebrate Paleontology*, **13**, 400–423.

Peng, G.-Z. 1992. Jurassic ornithopod *Agilisaurus louderbacki* (Ornithopoda:Fabrosauridae) from Zigong, Sichuan, China. *Vertebrata PalAsiatica* **30**(1), 39–51. [In Chinese with English summary.]

Perle, A., Maryánska, T. & Osmólska, H. 1982. *Goyocephale lattimorei* gen. et sp. n., a new flat-headed pachycephalosaur (Ornithischia, Dinosauria) from the Upper Cretaceous of Mongolia. *Acta Palaeontologica Polonica*, **27**, 115–127.

Pol, D., Rauhut, O. W. & Becerra, M. 2011. A Middle Jurassic heterodontosaurid dinosaur from Patagonia and the evolution of heterodontosaurids. *Naturwissenschaften*, **98**(5), 369–379.

Reig, O. A. 1963. La presencia de dinosaurios saurisquios en los 'Estrados de Ischigualasto' (Mesotriásico superior) de las Provincias de San Juany La Rioja (Republica Argentina). *Ameghiniana*, **3**, 3–20.

Romer, A. S. 1972. The Chañares (Argentina) Triassic reptile fauna. XV: Further remains of the thecodonts *Lagerpeton* and *Lagosuchus*. *Breviora*, **394**, 1–7.

Salgado, L., Canudo, J. I., Garrido, A. C., Morenoazanza, M., Martínez, L. C., Coria, R. A. & Gasca, J. M. 2017. A new primitive Neornithischian dinosaur from the Jurassic of Patagonia with gut contents. *Scientific Reports*, **7**, 42778.

Santa Luca, A. P. 1980. The postcranial skeleton of *Heterodontosaurus tucki* (Reptilia, Ornithischia) from the Stormberg of South Africa. *Annals of the South African Museum*, **79**(7), 159–211.

Seeley, H. G. 1887. On the classification of the fossil animals commonly named Dinosauria. *Proceedings of the Royal Society*, **43**, 165–171.

Sereno, P. C. 1986. Phylogeny of the bird-hipped dinosaurs (Order Ornithischia). *National Geographic Research*, **2**(2), 234–256.

Sereno, P. C. 1987. *The ornithischian dinosaur* Psittacosaurus *from the Lower Cretaceous of Asia and the relationships of the Ceratospia*. Unpublished PhD thesis, Columbia University, 544 pp.

Sereno, P. C. 1990. Psittacosauridae. Pp. 579–592 in D. B. Weishampel, P. Dodson & H. Osmólska (eds) *The Dinosauria*. 1st edition. University of California Press, Berkeley.

Sereno, P. C. 1991. *Lesothosaurus*, 'Fabrosaurids', and the early evolution of Ornithischian. *Journal of Vertebrate Paleontology*, **11**, 168–197.

Sereno, P. C. 1994. The pectoral girdle and forelimb of the basal theropod *Herrerasaurus ischigualastensis*. *Journal of Vertebrate Paleontology*, **13**, 425–450.

Sereno, P. C. 1999. The evolution of dinosaurs. *Science*, **284**, 2137–2147.

Sereno, P. C. 2000. The fossil record, systematics and evolution of pachycephalosaurs and ceratopsians from Asia. Pp. 480–516 in M. Benton, M. Shishkin, D. Unwin & E. Kurochkin (eds) *The age of dinosaurs in Russia and Mongolia*. Cambridge University Press, Cambridge.

Sereno, P. C. 2010. Taxonomy, cranial morphology, and relationships of parrot-beaked dinosaurs (Ceratopsia: *Psittacosaurus*). Pp. 21–58 in M. J. Ryan, B. J. Chinnery-Allgeier, D. A. Eberth & P. E. Ralrick (eds) *New perspectives on horned dinosaurs*. Indiana University Press, Bloomington.

Sereno, P. C. 2012. Taxonomy, morphology, masticatory function and phylogeny of heterodontosaurid dinosaurs. *ZooKeys*, **226**, 1–225.

Sereno, P. C. & Arcucci, A. B. 1994. Dinosaurian precursors from the Middle Triassic of Argentina: *Marasuchus*

lilloensis, gen. nov. *Journal of Vertebrate Paleontology*, **14**, 53–73.

Sereno, P. C., Martínez, R. N. & Alcober, O. A. 2013. Osteology of *Eoraptor lunensis* (Dinosauria, Sauropodomorpha). *Journal of Vertebrate Paleontology*, **32**(Supp. 6), 83–179.

Sternberg, C. M. 1951. Complete skeleton of *Leptoceratops gracilis* Brown from the Upper Edmonton Member on Red Deer River. *National Museum of Canada Bulletin, Annual Report (1949–50)*, **123**, 225–255.

Sues, H. D. & Galton, P. 1982. The systematic position of *Stenopelix Valdensis* (Reptilia: Ornithischia) from the Wealden of north-western Germany. *Palaeontographica Abteilung A*, **178**(4–6), 183–190.

Vickaryous, M. K., Maryańska, T. & Weishampel, D. B. 2004. Ankylosauria. Pp. 363–392 in D. B. Weishampel, P. Dodson & H. F. Osborn (eds) *The Dinosauria*. 2nd edition. University of California Press, Berkeley.

Weishampel, D. B. & Heinrich, R. E. 1992. Systematics of Hypsilophodontidae and basal Iguanodontia (Dinosauria: Ornithopoda). *Historical Biology*, **6**, 159–184.

Weishampel, D. B., Jianu, C. M., Csiki, Z. & Norman, D. B. 2003. Osteology and phylogeny of *Zalmoxes* (n.g.), an unusual euornithopod dinosaur from the latest Cretaceous of Romania. *Journal of Systematic Palaeontology*, **1**, 65–123.

Xu, X., Forster, C. A., Clark, J. M. & Mo, J. 2006. A basal ceratopsian with transitional features from the Late Jurassic of northwestern China. *Proceedings of the Royal Society, Series B*, **273**, 2135–2140.

Xu, X., Makovicky, P. J., Wang, X.-L., Norell, M. A. & You, H.-L. 2002. A ceratopsian dinosaur from China and the early evolution of Ceratopsia. *Nature*, **416**, 314–317.

You, H.-L. & Dodson, P. 2003. Redescription of neoceratosian dinosaur *Archaeoceratops* and early evolution of Neoceratopsia. *Acta Palaeontologica Polonica*, **48**, 261–272.

You, H.-L. & Dodson, P. 2004. Basal Ceratopsia. Pp. 478–493 in D. B. Weishampel, P. Dodson & H. Osmólska (eds) *The Dinosauria*. 2nd edition. University of California Press, Berkeley.

Zhao, X.-J., Cheng, Z.-W. & Xu, X. 1999. The earliest ceratopsian from the Tuchengzi Formation of Liaoning, China. *Journal of Vertebrate Paleontology*, **19**, 681–691.

Zhao, X.-J., Cheng, Z.-W., Xu, X. & Makovicky, P. J. 2006. A new ceratopsian from the Upper Jurassic Houcheng Formation of Hebei, China. *Acta Geologica Sinica*, **80**, 467–473.

Zheng, W.-J., Jin, X.-S. & Xu, X. 2015. A psittacosaurid-like basal neoceratopsian from the Upper Cretaceous of central China and its implications for basal ceratopsian evolution. *Scientific Reports*, **5**, 14190.